

Small-Scale Testing of Plutonium(IV) Oxalate Precipitation and Calcination to Plutonium Oxide to Support the MOX Feed Mission

M. L. Crowder
R. A. Pierce
J. H. Scogin
W. E. Daniel
W. D. King

June 2012

Savannah River National Laboratory
Savannah River Nuclear Solutions, LLC
Aiken, SC 29808

Prepared for the U.S. Department of Energy under
contract number DE-AC09-08SR22470.



DISCLAIMER

This work was prepared under an agreement with and funded by the U.S. Government. Neither the U.S. Government or its employees, nor any of its contractors, subcontractors or their employees, makes any express or implied:

1. warranty or assumes any legal liability for the accuracy, completeness, or for the use or results of such use of any information, product, or process disclosed; or
2. representation that such use or results of such use would not infringe privately owned rights; or
3. endorsement or recommendation of any specifically identified commercial product, process, or service.

Any views and opinions of authors expressed in this work do not necessarily state or reflect those of the United States Government, or its contractors, or subcontractors.

Printed in the United States of America

**Prepared for
U.S. Department of Energy**

Keywords: *Example keywords*

Retention: *Permanent*

Small-Scale Testing of Plutonium(IV) Oxalate Precipitation and Calcination to Plutonium Oxide to Support the MOX Feed Mission

M. L. Crowder
R. A. Pierce
J. H. Scogin
W. E. Daniel
W. D. King

June 2012

Savannah River National Laboratory
Savannah River Nuclear Solutions, LLC
Aiken, SC 29808

Prepared for the U.S. Department of Energy under
contract number DE-AC09-08SR22470.



REVIEWS AND APPROVALS

AUTHORS:

M. L. Crowder, Separation & Actinide Science Programs	Date
---	------

R. A. Pierce, Separation & Actinide Science Programs	Date
--	------

J. H. Scogin, Separation & Actinide Science Programs	Date
--	------

W. E. Daniel, Engineering Process Development	Date
---	------

W. D. King, Advanced Characterization & Processing	Date
--	------

TECHNICAL REVIEW:

K. M. L. Taylor-Pashow, Reviewer, Separation & Actinide Science Programs	Date
--	------

J. E. Therrell, Reviewer, HB-Line Engineering	Date
---	------

APPROVAL:

S. D. Fink, Manager Separation & Actinide Science Programs	Date
---	------

S. L. Marra, Manager Environmental & Chemical Process Technology Research Programs	Date
---	------

K. P. Burrows, Manager HB-Line Engineering	Date
---	------

ACKNOWLEDGEMENTS

The authors acknowledge excellent analytical support from David Missimer for particle size analysis, David DiPrete, Cecilia DiPrete and Mira Malek for radiochemical analysis, Mark Jones for ICPMS analysis, Boyd Wiedenman for ICPEs analysis, Tom White for ion chromatography analysis, and Amy Ekechukwu for acid analysis.

As lead author, I thank my co-authors for their key contributions, but recognize that I bear responsibility for inadequacies in this report.

In addition, I acknowledge the helpfulness of Jon Duffey and Eddie Kyser in technical discussions and experimental planning and Sam Fink in recruiting great teammates and providing wise technical and project guidance.

EXECUTIVE SUMMARY

The H-Canyon facility will be used to dissolve Pu metal for subsequent purification and conversion to plutonium dioxide (PuO_2) using Phase II of HB-Line. To support the new mission, SRNL conducted a series of experiments to produce calcined plutonium (Pu) oxide and measure the physical properties and water adsorption of that material. This data will help define the process operating conditions and material handling steps for HB-Line.

An anion exchange column experiment produced 1.4 L of a purified 52.6 g/L Pu solution. Over the next nine weeks, seven Pu(IV) oxalate precipitations were performed using the same stock Pu solution, with precipitator feed acidities ranging from 0.77 M to 3.0 M nitric acid and digestion times ranging from 5 to 30 minutes. Analysis of precipitator filtrate solutions showed Pu losses below 1% for all precipitations. The four larger precipitation batches matched the target oxalic acid addition time of 44 minutes within 4 minutes. The three smaller precipitation batches focused on evaluation of digestion time and the oxalic acid addition step ranged from 25-34 minutes because of pump limitations in the low flow range.

Following the precipitations, 22 calcinations were performed in the range of 610 – 690 °C, with the largest number of samples calcined at either 650 or 635 °C. Characterization of the resulting PuO_2 batches showed specific surface areas in the range of 5-14 m^2/g , with 16 of the 22 samples in the range of 5-10 m^2/g . For samples analyzed with typical handling (exposed to ambient air for 15-45 minutes with relative humidities of 20-55%), the moisture content as measured by Mass Spectrometry ranged from 0.15 to 0.45 wt % and the total mass loss at 1000 °C, as measured by TGA, ranged from 0.21 to 0.58 wt %. For the samples calcined between 635 and 650 °C, the moisture content without extended exposure ranged from 0.20 to 0.38 wt %, and the TGA mass loss ranged from 0.26 to 0.46 wt %. Of these latter samples, the samples calcined at 650 °C generally had lower specific surface areas and lower moisture contents than the samples calcined at 635 °C, which matches expectations from the literature.

Taken together, the TGA-MS results for samples handled at nominally 20-50% RH, without extended exposure, indicate that the Pu(IV) oxalate precipitation process followed by calcination at 635-650 °C appears capable of producing PuO_2 with moisture content < 0.5 wt % as required by the 3013 Standard.

Exposures of PuO_2 samples to ambient air for 3 or more hours generally showed modest mass gains that were primarily gains in moisture content. These results point to the need for a better understanding of the moisture absorption of PuO_2 and serve as a warning that extended exposure times, particularly above the 50% RH level observed in this study will make the production of PuO_2 with less than 0.5 wt % moisture more challenging. Samples analyzed in this study generally contained approximately 2 monolayer equivalents of moisture.

In this study, the bulk of the moisture released from samples below 300 °C, as did a significant portion of the CO_2 . Samples in this study consistently released a minor amount of NO in the 40-300 °C range, but no samples released CO or SO_2 . TGA-MS results also showed that MS moisture content accounted for 80±8% of the total mass loss at 1000 °C measured by the TGA.

The PuO_2 samples produced had particles sizes that typically ranged from 0.2 – 88 μm , with the mean particle size ranging from 6.4 – 9.3 μm . The carbon content of ten different calcination batches ranged from 190-480 $\mu\text{g C/g Pu}$, with an average value of 290 $\mu\text{g C/g Pu}$.

A statistical review of the calcination conditions and resulting SSA values showed that in both cases tested, calcination temperature had a significant effect on SSA, as expected from literature data. The statistical review also showed that batch size had a significant effect on SSA, but the narrow range of batch sizes tested is a compelling reason to set aside that result until tests with larger batch sizes are completed. When feed acidity was not included as a variable, calcination time had a significant effect on SSA. However, including feed acidity as a variable showed that neither feed acidity nor calcination time had a significant effect on SSA in this study. Also, for both cases the statistical review also indicated that digestion time did not have a significant effect on SSA.

TABLE OF CONTENTS

LIST OF TABLES	ix
LIST OF FIGURES	x
LIST OF ABBREVIATIONS	xii
1.0 Introduction	1
2.0 Experimental Procedure	2
2.1 Plutonium Purification by Anion Exchange	2
2.1.1 Column Description	2
2.1.2 Plutonium Feed Solutions	2
2.1.3 Column Operation	3
2.1.4 Characterization	3
2.2 Precipitation	3
2.3 Calcination	4
2.3.1 Batch 1 Calcinations	4
2.3.2 Calcination of Additional Batches	5
2.4 Thermocouple Evaluation	6
2.5 Characterization	6
3.0 Results and Discussion	7
3.1 Plutonium Purification by Anion Exchange	7
3.2 Precipitation	9
3.3 Calcination	9
3.4 Thermocouple Evaluation	11
3.5 Characterization	12
3.5.1 Descriptive Results	12
3.5.2 Moisture Analysis by TGA-MS	14
3.5.3 Carbon Analysis	17
3.5.4 Characterization Highlights	17
3.5.5 Particle Size Analysis	20
3.6 Review of Moisture Analyses	20
3.7 Statistical Analyses	22
4.0 Conclusions	24
5.0 Recommendations	25
6.0 References	26

LIST OF TABLES

Table 2-1. BET Specific Surface Area for NpO_2 .	4
Table 2-2. Target Calcination Conditions for Pu Oxalate Batches.	5
Table 3-1. Impurity Contents of Pu Product Solution	8
Table 3-2. Precipitation Conditions	9
Table 3-3. Precipitation Results	9
Table 3-4. Mass Changes during Calcination	10
Table 3-5. Glovebox Conditions after Calcination	11
Table 3-6. Thermocouple Evaluation Results	12
Table 3-7. Carbon Contents of PuO_2 Samples	17
Table 3-8. Characterization Highlights of Calcination Batches 1-3	18
Table 3-9. Characterization Highlights of Additional Calcination Batches	19
Table 3-10. Particle Size Analyses of PuO_2 Samples	20
Table 3-11. Particle Size Analyses of Pu Oxalate Samples	20
Table 3-12. Relations Between MS Moisture, TGA, and SSA	21
Table 3-13. Summary of Data for Statistical Analysis	22
Table 3-14. Statistical Summary of Fit – Case 1: All Data, 4 Parameters	23
Table 3-15. Statistical Parameter Estimate – Case 1: All Data, 4 Parameters	23
Table 3-16. Statistical Summary of Fit – Case 2: Omit Batch 1 Data, 5 Parameters	23
Table 3-17. Statistical Parameter Estimate – Case 2: Omit Batch 1 Data, 5 Parameters	23
Table A-1. Anion Exchange Results for Pu and Am	A-2
Table A-2. Impurity Contents in Anion Exchange Feed by ICPES	A-2
Table A-3. Uncertainties in MS Moisture Contents	A-4
Table A-4. Specific Surface Area Measurements with Uncertainties	A-5

LIST OF FIGURES

Figure 2-1. Crucible Holder Used for Calcinations.....	5
Figure 3-1. Pu and ²⁴¹ Am Released from Resin Column	7
Figure 3-2. Typical PuO ₂ Sample after Calcination	12
Figure 3-3. Typical SEM Results for PuO ₂	13
Figure 3-4. Typical SEM Results for Pu Oxalate	13
Figure 3-5. TGA Mass Measurements for Sample B3-1a	14
Figure 3-6. MS Signals (linear scale) from TGA-MS Analysis of Sample B3-1a	14
Figure 3-7. MS Signals (logarithmic scale) from TGA-MS Analysis of Sample B3-1a	15
Figure 3-8. MS Signals (linear scale) from TGA-MS Analysis of Sample B4-1b	16
Figure 3-9. MS Signals (logarithmic scale) from TGA-MS Analysis of Sample B4-1b	16
Figure A-1. MS Signals (linear scale) from TGA-MS Analysis of Sample D30-A	A-3
Figure A-2. MS Signals (logarithmic scale) from TGA-MS Analysis of Sample D30-A	A-3
Figure B-1. Temperature Profiles for Batch 1 Calcinations	A-7
Figure B-2. Temperature Profiles for Batch 2a Calcinations	A-7
Figure B-3. Temperature Profiles for Batch 2b Calcinations	A-8
Figure B-4. Temperature Profiles for Batch 3-1 Calcinations	A-8
Figure B-5. Temperature Profiles for Batch 3-2 Calcinations	A-9
Figure B-6. Temperature Profiles for Batch 3-3 Calcinations	A-9
Figure B-7. Temperature Profiles for Batch 3-4 Calcinations	A-10
Figure B-8. Temperature Profiles for Batch 3-5 Calcinations	A-10
Figure B-9. Temperature Profiles for Batch 4 Calcinations	A-11
Figure B-10. Temperature Profiles for Batch D5 Calcinations	A-11
Figure B-11. Temperature Profiles for Batch D30-A Calcinations	A-12
Figure B-12. Temperature Profiles for Batch D30-B Calcinations	A-12
Figure B-13. Temperature Profiles for Batch D15-A Calcinations	A-13
Figure B-14. Temperature Profiles for Batch D15-B Calcinations	A-13

Figure C-1. Particle Size Analysis for Batch 1 PuO ₂	A-15
Figure C-2. Particle Size Analysis for Batch 3 PuO ₂	A-16
Figure C-3. Particle Size Analysis for Batch 4 PuO ₂	A-17
Figure C-4. Particle Size Analysis for Batch D5-A PuO ₂	A-18
Figure C-5. Particle Size Analysis for Batch D5-B PuO ₂	A-19
Figure C-6. Particle Size Analysis for Batch D30 PuO ₂	A-20
Figure C-7. Particle Size Analysis for Batch D15 PuO ₂	A-21
Figure C-8. Particle Size Analysis for Batch 2 Pu Oxalate	A-22
Figure C-9. Particle Size Analysis for Batch 4 Pu Oxalate	A-23
Figure C-10. Particle Size Analysis for Batch D5 Pu Oxalate	A-24
Figure C-11. Particle Size Analysis for Batch D30 Pu Oxalate	A-25
Figure C-12. Particle Size Analysis for Batch D15 Pu Oxalate	A-26

LIST OF ABBREVIATIONS

ANN	aluminum nitrate nonahydrate
BET	Brunauer-Emmett-Teller
BV	bed volume
DI	deionized water
IC	ion chromatography
ICP-ES	inductively coupled plasma emission spectroscopy
ICP-MS	inductively coupled plasma mass spectroscopy
MOX	Mixed Oxide
PHA	pulse height analysis
PSA	particle size analysis
RH	relative humidity
SEM	scanning electron microscopy
SRNL	Savannah River National Laboratory
SSA	specific surface area
TGA-MS	thermogravimetric analysis-mass spectrometry

1.0 Introduction

H-Canyon and HB-Line are tasked with the production of plutonium oxide (PuO_2) from a feed of plutonium metal. The PuO_2 will provide feed material for the Mixed Oxide (MOX) Fuel Fabrication Facility. After dissolution of the Pu metal in H-Canyon, plans are to transfer the solution to HB-Line for purification by anion exchange, followed by plutonium(IV) oxalate precipitation, filtration and calcination to form PuO_2 . This report details the results from SRNL precipitation, filtration, calcination and characterization tests, as requested by HB-Line¹ and described in the task plan².

H-Area Engineering selected direct strike Pu(IV) oxalate precipitation³ mainly because it yields a denser PuO_2 product than Pu(III) oxalate precipitation. The term “direct strike” indicates that the oxalic acid is added to a tank already containing Pu solution. The Pu(IV) approach also eliminates the need for reduction by ascorbic acid. The proposed HB-Line precipitation process^{1,2} involves a digestion time of 5 minutes after the time required for oxalic acid addition, as was used during HB-line production of neptunium oxide (NpO_2). Therefore, in this study, researchers targeted an oxalic acid addition time of 44 minutes to match expected HB-Line conditions. In addition, a series of small Pu(IV) oxalate precipitation tests with different digestion times were conducted to better understand the effect of digestion time on particle size, filtration efficiency and other factors.

After production in HB-Line, plans are to ultimately store the purified PuO_2 in containers suitable for compliance with the DOE-STD-3013 (i.e., the 3013 Standard).⁴ Originally, the Standard required heating of plutonium materials to 950 °C for 2 hours in air, with a resulting moisture content of less than 0.5 wt %. Later, the 3013 Standard allowed stabilization at 750 °C for 2 hours in air for materials with high chloride salt content, thus reducing the volatilization of chloride salts during stabilization. It is expected that the results of this study will be included as part of a technical basis requesting that the 3013 Standard be modified to allow certain purified PuO_2 materials to be calcined at low temperature conditions, such as 640 - 650 °C for 3-4 hours. Though the available technical literature helps understand the effects of calcination temperature and time on specific surface area (SSA) for PuO_2 , most of these studies have calcined PuO_2 at different temperatures than expected in current HB-Line furnaces. One helpful publication from Los Alamos National Laboratory⁵ showed that production of PuO_2 by Pu(IV) oxalate precipitation and subsequent calcination at 650 °C for 4 hours consistently produced PuO_2 with a specific surface area of $9.77 \pm 1.79 \text{ m}^2/\text{g}$ and moisture content of $0.22 \pm 0.08 \text{ wt } \%$. However, a literature review⁶ of PuO_2 calcination studies showed a need for additional data in the temperature range of interest, 600-650 °C. In addition, the review showed that the SSA of PuO_2 changes significantly with calcination temperature in the temperature range of interest, and the lower the SSA, the less likely the PuO_2 is to absorb moisture.

In light of the need for more data pertinent to the expected process conditions, researchers performed a set of calcination tests at different times and temperatures that are achievable in current HB-Line equipment. The calcined batches of PuO_2 were characterized for moisture and SSA, since moisture is already a requirement in the 3013 Standard, and SSA provides an indication of how much water would be re-adsorbed onto PuO_2 when exposed to humid air.

In addition, since the 3013 Standard requires that the calcination (or stabilization) process eliminate organics, characterization of PuO_2 batches monitored the presence of oxalate, by thermogravimetric analysis-mass spectrometry (TGA-MS). To use the TGA-MS for carbon or oxalate content, some method development will be required. However, the TGA-MS is already used for moisture measurements. Therefore, SRNL initiated method development for the TGA-MS to allow quantification of oxalate or total carbon. That work continues at this time and is not

yet ready for use in this study although the collected test data can be reviewed later as those analysis tools are available. In the current report, the TGA-MS provides a “less than” quantity for oxalate, since total mass loss and moisture loss is readily quantified.

2.0 Experimental Procedure

2.1 Plutonium Purification by Anion Exchange

2.1.1 *Column Description*

To perform Pu(IV) oxalate precipitation tests, researchers prepared a purified Pu solution by anion exchange. The ion exchange column was fabricated from 90-mm borosilicate glass tubing (1.5-mm wall thickness) by the SRNL Glass Shop. A coarse frit was sealed into the bottom of the column to hold the resin. Approximately 1.6 L of Reillex™ HPQ anion exchange resin were loaded into the column for a bed height of ~27 cm. Solutions were fed to the column from the top and effluent was withdrawn from the bottom. Solutions were fed to the column using a FMI QV-50 piston pump. Polyethylene tubing (6.35 mm outside diameter) linked feed bottles, effluent collection bottles, and the pump to the column.

2.1.2 *Plutonium Feed Solutions*

Feed solutions came from two source materials. The first feed source was δ -phase Pu metal dissolved using 8-10 M nitric acid (HNO_3), potassium fluoride (KF), and either gadolinium (Gd) or boron (B).⁷ The second feed source was a mixed PuO_2 batch (termed HBL-11-OX8 or 3013 DE Feed) that was fused with sodium peroxide and dissolved in 8 M HNO_3 . The 3013 DE Feed contained impurities that are listed in Appendix A. The material from the two feed sources was further divided into separate feed solutions, as listed below.

- 1) 4.4 L of dissolved HBL-11-OX8 material (3013 DE Feed). The solution contained ~42.1 g of Pu. The total NO_3^- concentration was ~8 M and the HNO_3 concentration was ~6.7 M. The solution was filtered through a 5-micron filter.
- 2) 1.0 L of dissolved δ -phase metal. The solution contained ~7.6 g of Pu. The solution concentrations were 10 M HNO_3 , ~0.075 M KF, and 1.0 g/L B. To this solution were added 84 mL of 2.0 M aluminum nitrate nonahydrate (ANN) solution to complex fluoride at a 2:1 Al:F molar ratio and 190 mL deionized (DI) water to reduce the total NO_3^- concentration. The solution was not filtered after the addition of ANN and DI H_2O .
- 3) 1.6 L of dissolved δ -phase metal. The solution contained ~7.5 g of Pu. The solution concentrations were 9.5 M HNO_3 , ~0.16 M KF, and 1.5 g/L B. To this solution were added 260 mL of 2.0 M ANN solution to complex fluoride at a 2:1 Al:F molar ratio and 190 mL DI water to reduce the total NO_3^- concentration. The solution was not filtered after the addition of ANN and DI H_2O .
- 4) 1.6 L of dissolved δ -phase metal. The solution contained ~11.5 g of Pu. The solution concentrations were 10.3 M HNO_3 , ~0.05 M KF, and 0.63 g/L Gd. To this solution were added 77 mL of 2.0 M ANN solution to complex fluoride at a 2:1 Al:F molar ratio and 250 mL de-ionized (DI) water to reduce the total NO_3^- concentration. The solution was not filtered after the addition of ANN and DI H_2O .
- 5) 1.7 L of dissolved δ -phase metal. The solution contained ~8.6 g of Pu. The solution concentrations were 9.3 M HNO_3 , ~0.044 M KF, and 0.67 g/L Gd. To this solution were added 80 mL of 2.0 M ANN solution to complex fluoride at a 2:1 Al:F molar ratio and 120 mL DI water to reduce the total NO_3^- concentration. The solution was not filtered after the addition of ANN and DI H_2O .

2.1.3 Column Operation

The ion exchange resin was conditioned, loaded, washed, and eluted with downward flow. Prior to loading Pu onto the resin, the column was conditioned with 4 L of 8 M HNO₃ at 90 mL/min. Feed #1 was fed at 60 mL/min. The column was then washed with 1.6 L of 8 M HNO₃ to harvest some of the ²⁴¹Am. Feeding of Pu continued with Feeds #2, #3, and #4 being processed at 60 mL/min.

During the loading of Feed #5, greatly reduced flow rates through the column were observed, most likely due to the presence of a precipitate. Parts of the unprocessed feed were mixed with 8 M HNO₃ wash solution and passed through the column. The solids causing the reduced processing rate dissolved and improved flow was re-established. However, due to time constraints, only half of Feed #5 was loaded onto the column.

After feeding was complete, the Pu on the column was washed with 7 L of 8 M HNO₃ at 60-90 mL/min. The Pu was eluted with 0.35 M HNO₃. The heads cut (1.2 L) was collected at a flow rate of 30 mL/min. The hearts cut (1.4 L) was obtained at 20 mL/min with a targeted Pu concentration of 50 g/L.

2.1.4 Characterization

The feed, product and other effluent solutions from the anion exchange column experiment were characterized by some or all of these methods: gamma pulse height analysis (PHA), inductively coupled plasma-mass spectroscopy (ICP-MS), inductively coupled plasma-emission spectroscopy (ICP-ES), ion chromatography (IC) for anions, and free acid. In addition, to attain lower detection limits and to reduce interferences for some impurities in the Pu product solution, the Pu product solution was analyzed by ICP-MS and ICP-ES after Pu removal. The details of that method development effort are documented elsewhere.⁸

2.2 Precipitation

The Pu product solution described above was stored and used for seven precipitation batches. No valence adjustments were performed before any of the precipitations. Precipitation tests began before acid analysis of the Pu product solution completed. For precipitations involving acid adjustments, researchers added the volume of 7 M HNO₃ needed to raise the solution to a target concentration of 2.5 M HNO₃ for Batch 4 or a target concentration of 1.5 M HNO₃ for Batches D-5, D-30 and D-15. Typically, precipitations began within about 2 h after acid adjustments. Free acid analyses occurred after precipitations completed. Prior to each precipitation batch, researchers calculated the volume of 0.9 M oxalic acid needed to achieve 0.1 M excess oxalic acid after Pu precipitation, and that volume of 0.9 M oxalic acid was transferred into a 250-mL bottle. For each precipitation, purified Pu solution was heated in a glass beaker to 50 ± 3 °C. Researchers used a 2-L glass beaker for the first three batches (nominally 18.5 g Pu each) and a 600-mL glass beaker for the smaller remaining batches (4-6 g Pu each). Once the Pu solution reached nominally 50 °C, 0.9 M oxalic acid was added at a flow rate that targeted a total oxalic acid addition time of 44 minutes, to correspond to expected HB-Line precipitation conditions.³ A summary of the precipitation conditions is provided in the Results section.

For the first three precipitation batches, the digestion time, or time between end of oxalic addition and start of filtration, was nominally 15 minutes. The fourth precipitation batch involved a digestion time of 6 minutes. Then, for the last three precipitations, the digestion times were 5, 30 and 15 minutes, so those batches are designated D-5, D-30 and D-15. Attempts were made to make all other experimental conditions consistent for these last three precipitations to determine the minimum digestion time and the effects of digestion time on oxalate and oxide properties.

Following each precipitation, the Pu oxalate slurry was poured into a stainless steel filter housing containing a nominally 10- μm stainless steel filter screen material provided by HB-Line. Prior to testing, the SRNL Glass Shop cut appropriately-sized circular sections of the filter screen, and prior to each filtration, personnel loaded a new filter into the filter housing and performed a leak check. After the bulk of the Pu oxalate slurry was transferred to the filter housing and the liquid was vacuum filtered and collected in a 1-L beaker, the Pu oxalate solids remaining in the glass beaker were transferred using modest volumes of cake wash solution (i.e., 1.4 M HNO_3 / 0.1 M oxalic acid), but additional cake washing did not occur. Except for Batch 1, the vacuum continued to operate for 15-60 minutes after standing liquid was gone from the cake. In addition, all oxalate batches except Batch 1 remained open to the ambient conditions overnight or longer to promote drying. Volumes used for each precipitation are shown in the Results section. Filtrate solutions were characterized by gamma PHA to allow determination of Pu losses to the filtrate. Filtrate solutions were also characterized by ICP-MS, ICP-ES and IC.

2.3 Calcination

2.3.1 *Batch 1 Calcinations*

The first precipitation batch of Pu oxalate, or $\text{Pu}(\text{C}_2\text{O}_4)_2 \cdot x\text{H}_2\text{O}$, was transferred to a 4-ounce (~110 mL) glass jar, which was then closed. Four days later, this Batch 1 material was divided into four 30-mL quartz crucibles (B1-2 through B1-5). The $\text{Pu}(\text{C}_2\text{O}_4)_2$ material was quite wet and sticky and difficult to transfer completely. Each crucible had a bed depth of approximately 2-3 cm. As noted in previous SRNL work⁹ with neptunium oxide (NpO_2) oxide calcinations, we assumed that a bed depth of 2-3 cm (or less for later in this study) would allow enough air to permeate the powder during calcination that the PuO_2 produced would be reasonably similar to that produced in HB-Line at similar conditions. This assumption seems reasonable because in the case of NpO_2 , the batches of NpO_2 calcined at SRNL at 600 and 650 °C for 2 hours had specific surface areas which bounded that of the NpO_2 made by HB-Line early in the production campaign as shown in Table 2-1.¹⁰

Table 2-1. BET Specific Surface Area¹⁰ for NpO_2

NpO_2 Material	BET Specific Surface Area, m^2/g
SRNL 600 °C	5.34
SRNL 650 °C	3.67
HB-Line	4.03

The HB-Line design, which passes air through the filter cake (or powder bed) during calcination, effectively removes moisture and oxalate decomposition products from the filter cake, and may have additional advantages for the properties of the PuO_2 .

Having assumed that a shallow bed depth without an air purge was reasonable, a thermocouple with a 0.5-mm diameter probe was inserted into each of the four cakes and the four crucibles were loaded into a Barnstead Thermolyne 1300 muffle furnace capable of heating to 1100 °C. Unfortunately, moving two of the crucibles to the back of the furnace caused the affected thermocouple probes to bend enough that the thermocouple tips were no longer in contact with the $\text{Pu}(\text{C}_2\text{O}_4)_2$ material. The thermocouples in the front two crucibles, however, were verified to be in contact with the cake at the start of calcination. After calcination above 600 °C for 2 h, the furnace door was opened to remove the first crucible. At that time, personnel observed that the thermocouples in the front two crucibles were no longer touching the cakes, but were positioned

just above the cakes. It appeared that the mass loss from drying and calcination of the oxalate to oxide caused the cake to subside enough that contact with the thermocouples was lost.

2.3.2 Calcination of Additional Batches

Batch 2 calcinations were performed with two crucibles in the furnace at a time with a target cake temperature of 625 °C. While calcining the first pair of samples, the cake temperatures were 625 °C (B2-4) and 628 °C (B2-5), and the samples were calcined for 4 and 5 h, respectively. Next, an additional pair of oxalate samples was calcined. In this case, however, the cake temperatures were 625 °C (B2-3) and 610 °C (B2-2) and the calcination times were 3 and 2 h, respectively. Because of the temperature variation observed within the furnace, the first four Batch 3 samples (B3-1 through B3-4) were calcined individually to ensure the desired cake temperature of 650 °C was attained. A summary of the calcination conditions is shown in Table 2-2. Thereafter, a firebrick crucible holder (shown in Figure 2-1) was used, along with smaller (15-mL) quartz crucibles. The expectation was that the crucible holder would reduce temperature variation within the furnace, and would also prevent the crucibles from tipping over.

Table 2-2. Target Calcination Conditions for Pu Oxalate Batches.

Batch	Target Pu g	Portions	Target Temp. °C	Crucible Holder Y or N
1	17.5	4	650	N
2	17.5	4	625	N
3	17.5	4	650	N
3		2	635	Y
4	6.36	2	635, 650	Y
D-5	4.21	2	635, 650	Y
D-30	4.21	2	635, 650	Y
D-15	4.86	2	635, 650	Y

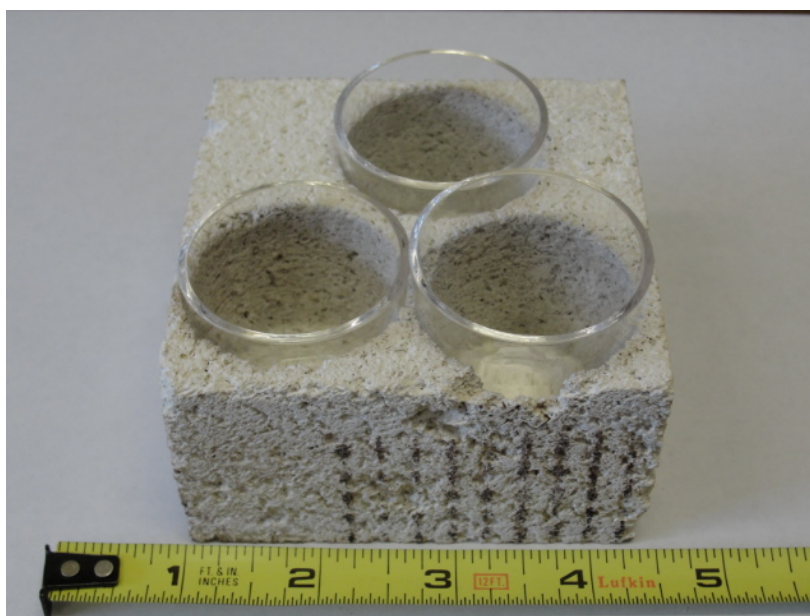


Figure 2-1. Crucible Holder Used for Calcinations.

2.4 Thermocouple Evaluation

In the Task Technical and Quality Assurance Plan set forth at the beginning of this study, personnel accepted the manufacturer's calibration of the thermocouples to be used. However, after significant temperature variations within the furnace were observed during Batch 1 calcinations, evaluations were made of the precision and accuracy of the four thermocouples used in this study. Prior to Batch 2 and the subsequent calcinations, the precision of the thermocouples near 650 °C was tested by placing all four thermocouples into an empty quartz crucible and heating the furnace. In addition, the four thermocouples were checked for precision at room temperature and were checked for precision and accuracy by measuring the temperature of boiling water. After the calcinations for this study were complete, the four thermocouples were again tested for precision by heating in the furnace to nominally 650 °C. However, in this case, the thermocouple probes were twisted together to ensure they were in essentially the same position. After that, a test for thermocouple accuracy was made by inserting one thermocouple into a thin hole drilled into a small aluminum cylindrical block. The cylinder was turned upside down and placed inside a quartz crucible, so that the thermocouple tip would remain inside the aluminum block. The other three thermocouples were left in the furnace and stationed in the same place but not in contact with the crucible. Then, the furnace was heated to above 700 °C to ensure melting of the aluminum, as pure aluminum melts at 660.6 °C. Throughout heating, the temperatures of the four thermocouples and the furnace thermocouple were recorded. Then the furnace was allowed to cool to ~600 °C and temperatures continued to be recorded. The furnace was heated above 700 °C, cooled below 600 °C then heated above 700 °C a third time in attempt to determine a consistent melting point of the aluminum block. The expectation was that during melting, the thermocouple in contact with the aluminum would have a slower rate of temperature change than it would before or after melting. Also, during cooling, the molten aluminum is expected to cool somewhat rapidly until solidification begins. However, after solidification, a higher rate of temperature decrease was expected. The aluminum alloy used was expected to be of the aluminum alloy type 6061, and it cut readily as compared to more pure aluminum alloys which are much softer. To confirm the alloy designation, a portion of the same aluminum rod was dissolved in 1 M hydrochloric acid and submitted for analysis by ICP-ES. Aluminum 6061 contains nominally 0.6 wt % silicon (Si), 1.0 wt % magnesium (Mg), 0.25 wt % copper (Cu), and 0.20 wt % chromium (Cr).¹¹

2.5 Characterization

The plutonium oxide (PuO₂) samples from all the batches and portions generated in this study were characterized by thermogravimetric analysis-mass spectrometry (TGA-MS) for moisture content and by the Brunauer-Emmett-Teller (BET) method for specific surface area (SSA). In addition, at least one oxide sample from each of the larger batches was evaluated by either Particle Size Analysis (PSA) or by Scanning Electron Microscopy (SEM). Note that the initial Task Plan² for this study did not include exposing PuO₂ samples to humid air. Thus, though exposures to humid air were performed in this study to provide indications of moisture absorption behavior, the humidity meters were out of calibration. An end of study comparison using a calibrated humidity meter showed a bias that is noted in the affected table.

For most batches, a sample of the Pu(C₂O₄)₂ was also evaluated for PSA and some samples were evaluated by SEM for morphology.

3.0 Results and Discussion

3.1 Plutonium Purification by Anion Exchange

Analysis of the hearts cut by ICP-MS measured 52.7 g/L for Masses 239-241 and a ^{239}Pu enrichment of 94.0%. Gamma spectroscopy analysis measured 49.4 g/L ^{239}Pu . Factoring for the enrichment measured by ICP-MS, the total Pu concentration determined using gamma spectroscopy was 52.6 g/L. Free acid analysis measured 0.77 M H^+ . Ion chromatography measurement reported fluoride < 10 mg/L, chloride < 10 mg/L and nitrate = 91.4 g/L (1.47 M). In this case, the analyses confirm one another. The gamma analysis of 52.6 g Pu/L converts to 0.22 M Pu. It is expected that the Pu is present as Pu(IV), which is associated with four nitrate ions per Pu ion, yielding 0.88 M nitrate complexing the Pu. Combining the free acid (nitric acid) result of 0.77 M with the 0.88 M nitrate complexing the Pu yields an expected total nitrate of 1.65 M. The ion chromatography analysis of total nitrate is within 12% of this prediction, at a value of 1.47 M nitrate.

Analytical results from the anion exchange column experiment are provided in Appendix A, and generally confirm expectations concerning resin performance. A plot of the Pu and ^{241}Am content of the solution exiting the resin column is shown in Figure 3-1, using average feed concentrations of 7.52 g Pu/L and 0.028 g Am/L for comparison. In Figure 3-1, the first bed volume (BV) of wash corresponds to a feed that was nominally a 50:50 mixture of feed and wash solution. Also in the figure, BV #5 refers to the Heads Cut and BV #6 is the Hearts Cut.

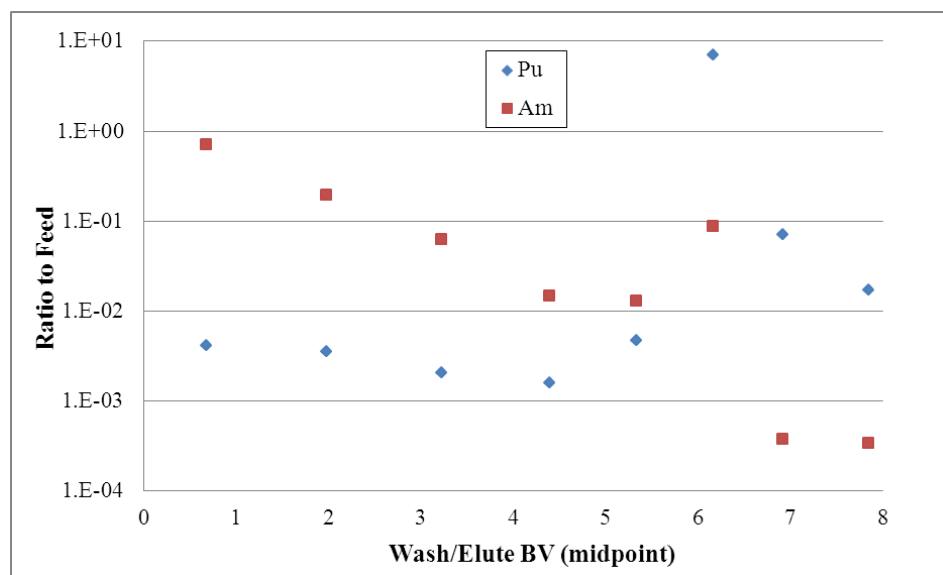


Figure 3-1. Pu and ^{241}Am Released from Resin Column

Though this experiment included only ~3.6 BV of wash, the Pu product solution was relatively pure, as shown in Table 3-1. To compare the impurity contents to the Column A Limits², the analysis results are color-coded in Table 3-1, where red indicates the limit was not attained. For two of the “red” analytes, potassium (K) and manganese (Mn), the solution showed less than the detection limit, but the limit was above the Column A specification. For analytes in which the

Column A limit was attained, the closeness to the limit is indicated, in order, by the colors yellow, white, and green. Yellow indicates an impurity concentration above 50% of specification. White indicates an impurity concentration between 10% and 50% of specification. Green indicates an impurity concentration below 10% of specification.

Table 3-1. Impurity Contents of Pu Product Solution

Element	Isotope Used By ICPMS	Column A Limit $\mu\text{g/g Pu}$	Measured $\mu\text{g/g Pu}$	% of Column A Limit
Al	--	500	< 33.5	< 6.7
B	--	100	< 28.9	< 28.9
Be	--	100	< 1.14	< 1.1
Ca	--	500	< 106	< 21.3
Cd	Cd-111	10	0.67	6.7
Cd	Cd-113	10	0.58	5.8
Co	Co-59	100	0.35	0.4
Cr	--	1000	< 19.4	< 1.9
Cu	--	100	< 40.9	< 40.9
Dy	Dy-163	1	0.38	38.3
Eu	Eu-151	1	0.073	7.3
Eu	Eu-153	1	0.11	11.3
F	--	250	< 190	< 76.0
Fe	--	2000	< 63	< 3.1
Ga	Ga-69	12000	0.88	0.01
Ga	Ga-71	12000	0.65	0.01
Gd	Gd-155	3	8.85	295
Gd	Gd-157	3	8.60	287
K	--	300	< 572	< 191
Li	--	400	< 27.8	< 6.9
Mg	--	500	< 91.3	< 18.3
Mn	--	100	< 101	< 101
Mo	--	100	< 51.0	< 51.0
Na	--	1000	< 303	< 30.3
Ni	--	5000	< 86.5	< 1.7
Pb	Pb-206	200	15.6	7.8
Pb	Pb-207	200	14.7	7.4
Pb	Pb-208	200	14.9	7.5
S	--	250	< 228	< 91.3
Si	--	200	< 186	< 92.9
Sm	Sm-147	2	0.40	20.2
Sm	Sm-149	2	0.21	10.4
Sn	Sn-118	100	4.07	4.1
Sn	Sn-120	100	4.12	4.1
Ti	--	100	< 3.61	< 3.6
V	--	300	< 22.2	< 7.4
Zn	--	150	< 17.5	< 11.7
Note: Red background indicates impurity concentration above specification. Yellow indicates impurity concentration above 50% of specification. White indicates impurity concentration between 10% and 50% of specification. Green indicates impurity concentration below 10% of specification.				
Note: Values from ICPMS are reported as elemental concentrations and have been corrected for natural abundance.				

3.2 Precipitation

A summary of precipitation conditions is shown below.

Table 3-2. Precipitation Conditions

Batch	52.6 g/L Pu mL	0.9 M Oxalic mL	7M HNO ₃ mL	Oxalic acid addition time, min	Digestion Time min	Wash Solution mL	Vacuum Drying Time min	Comments
1	351	239	0	43	17	118	< 10	Oxalate wet and pasty
2	348	234	0	48	13	149	40	
3	352	240	0	45	15	114	30-60	
4	120	87	46	44	6	48	~24	
D-5	80	56	10.4	34 [†]	5	65	15	
D-30	80	56	10.4	25 [†]	30	63	42	Oxalate wet and pasty
D-15	60+45*	67	15.8	34 [†]	15	73	~30	

* 45 mL of ~1.5 M HNO₃ containing ~1.7 g Pu were added.

[†] The target addition time of 44 minutes was not attained because the low flow rate required was just below the minimum flow rate of the pump.

Note for all Batches except Batch 1, the Pu oxalate cake was kept open overnight, allowing additional drying. For Batch 3, the weights of the Pu oxalate cake were recorded before and after air drying overnight, and a 2% mass loss occurred.

Table 3-3. Precipitation Results

Batch	Pu g	Pu Oxalate g	Pu in Filtrate [†] g	% Pu Losses to Filtrate
1	18.5	41.58*	0.156	0.84
2	18.3	48.07	0.105	0.57
3	18.5	51.44	0.107	0.58
4	6.31	14.26	0.0243	0.39
D-5	4.21	11.20	0.0204	0.48
D-30	4.21	12.16	0.0280	0.67
D-15	4.86	11.89	0.0213	0.44

* Spills occurred during Batch 1 operations.

[†] Determined by gamma PHA with isotopic ratio by ICPMS.

After the Batch 3 precipitation, personnel noted the position of the Pu oxalate cake in the filter apparatus. Following removal of the Pu oxalate and cleaning of the filter apparatus, the approximate volume of the filter cake was determined by filling the filter apparatus with water to the same fill level as the filter cake had been. Researchers determined the filter cake volume was ~40 mL. Since Batch 3 contained 18.5 g Pu, the density of Pu in the precipitate filter cake was deemed ~0.4 - 0.5 g Pu/mL cake.

3.3 Calcination

Using calcination temperatures ranging from 610 to 690 °C, the Pu(C₂O₄)₂•xH₂O samples were converted to PuO₂. For the nine calcinations involving Batch 1-4 materials, Appendix B provides

furnace and sample temperature profiles. Table 3-4 shows the masses of the initial oxalate material prior to calcination and the mass of the resulting PuO₂ product, along with the expected theoretical, dry amounts. Taking an average of all the batches except Batch 1, the PuO₂ mass was about 41% of the initial oxalate mass, which indicates that the Pu(C₂O₄)₂ cake was typically quite wet, having more than ten waters of hydration. Losses are attributed to minor spills during operations. Batches were precipitated from the same, purified Pu stock solution.

Table 3-4. Mass Changes during Calcination

Batch	Pu in Feed g	Pu Oxalate (Theory) g	Pu Oxalate (Actual) g	PuO ₂ (Theory) g	PuO ₂ (Actual) g [†]
1	18.5	32.1	41.58*	21.0	14.32*
2	18.3	31.8	48.07	20.8	19.22
3	18.5	32.1	51.44	21.0	20.72
4	6.31	11.0	14.26	7.2	6.61
D-5	4.21	7.3	11.20	4.8	4.55
D-30	4.21	7.3	12.16	4.8	4.64
D-15	4.86	8.4	11.89	5.5	5.22

* Spills occurred during Batch 1 operations.

[†] These values reflect total product recovered, not including SEM samples.

After calcination for the specified time, the quartz crucible was removed from the furnace at temperature and covered with a non-sealing quartz lid. After a brief cooling period, as shown in Table 3-5, the resulting PuO₂ was transferred into a glass vial, which was immediately covered with a lid then placed into a secondary plastic bottle with a lid to minimize exposure to humid air. Exposure times are also provided in Table 3-5, along with ambient glovebox conditions.

Table 3-5. Glovebox Conditions after Calcination

Calcination Batch	Glovebox Conditions during Cooling		Time for Cooling and Transfer into Vial	Comments
	T °C	RH %	min	
B1	NM	NM	~30 min	B1-2 crucible lid not used during cooling
B2-4	23.1	20.9	45 min	
B2-5	21.6	24.0	16 hours	
B2-2, B2-3	20.0	31.3	~30 min	
B3-1	24.0	43.2	34 min	
B3-2	23.4	41.0	17 min	Crucible lid not used
B3-3	24.9	45.7	19 min	
B3-4	24.0	50.9	22 min	
B3-5B	24.0	47.2	13 min	
B3-5A			18 min	
B4-1	21.7	32.0	15 min	
B4-2			12 min	
D5-B	23.2	52.3	10 min	
D5-A			10 min	
D30-A	23.0	50.0	13 min	
D30-B	25.4	30.1	~13 min	
D15-A	21.9	28.9	~25 min	
D15-B	24.0	26.0	~20 min	

NM = not measured

3.4 Thermocouple Evaluation

The four thermocouples used in this study were subjected to several evaluations for precision and accuracy. The thermocouple probes were all new at the beginning of the study. Two nearly identical thermocouple temperature readouts from Digi-Sense were used (one labeled DualLogR™ and the other Dual JTEK), each displaying the temperature of two thermocouples. The readout used for thermocouples T1 and T2 had been calibrated for the 0-200 °C range as M&TE # ATD1-400, with the calibration valid through 28 July 2012. Table 3-6 below shows the results of the different evaluations. As shown in the Table 3-6, the thermocouples reported temperatures with a standard deviation of ± 3 °C in the temperature range above 600 °C (measurements of greatest interest are in bold). Also, the test for an accurate melting temperature of an Al block showed that the start of solidification was clear because the temperature abruptly stopped decreasing for several minutes. The first “end of melting” temperature is not included because temperature readings were too variable. After that initial melting, solidification of the Al started at 653 °C for both cycles measured. This solidification temperature agrees well with the top of published melting range for the expected alloy, Aluminum 6061, which is 582.2 – 651.7 °C.¹² Recall that Aluminum 6061 contains nominally 0.6 wt % silicon (Si), 1.0 wt % magnesium (Mg), 0.25 wt % copper (Cu), and 0.20 wt % chromium (Cr).¹¹ Analysis of impurities in a sample of dissolved Al block by ICPES showed 0.68 wt % Mg, 1.0 wt % Si, which matches the nominal concentrations of Aluminum 6061. The dissolved sample also showed 0.08 wt % Cr, which is below the nominal level but clearly a component of the material. The dissolved sample also showed 0.005 wt % Cu which is attributed to the fact that CuCl₂ is sparingly soluble in water and the dissolution reaction was taken to completion, consuming chloride ion that would have been available to complex the Cu ions. The lead author’s review of the contents of 44 common aluminum alloys¹¹ showed that Aluminum 6061 is still the most likely

alloy used in the furnace evaluation, and the only other common alloy with 0.6 wt % Mg and 1.0 wt% Si, Aluminum 6262, has the same melting range as Aluminum 6061.¹² Therefore, the thermocouples used in this study showed sufficient precision (± 3 °C at 1 standard deviation) and sufficient accuracy (measuring boiling water and the melting point of an aluminum alloy) to provide reliable calcination temperatures.

Table 3-6. Thermocouple Evaluation Results

Time	Condition	T ₁ °C	T ₂ °C	T ₃ °C	T ₄ °C
Prior to Batch 2	Ambient	19.8	19.9	19.6	19.7
Prior to Batch 2	In furnace @ 670 °C	657.7*	657.4*	665.3*	664.5*
Prior to Batch 2	Ambient	20.1	20.2	19.8	19.9
Prior to Batch 2	Boiling Water	99.7	99.9	99.3	99.6
After Calcinations Complete	Ambient	19.5	19.7	19.3	19.4
	In furnace @ 699 °C [†]	675.9	678.2	675.4	671.3
	In furnace @ 777 °C [†]	754.3	756.4	753.6	750.0
After Calcinations Complete [#]	Start of 1 st solidification of Al	653	(647)	(647)	(645)
	End of 2 nd Al melting	~654	(737)	(736)	(729)
	Start of 2 nd solidification of Al	653	(651)	(651)	(650)
	End of 3 rd Al melting	~658	(747)	(746)	(738)

*Post-evaluation inspection showed that T₁ and T₂ were nearly touching each other and were at the bottom of the crucible. The tips of thermocouples T₃ and T₄ were both about halfway up the crucible, not touching each other and T₄ was not touching the crucible. All temperatures were still rising slowly.

[†] Thermocouple temperatures still increasing slowly when temperatures recorded.

[#] Only T₁ was in contact with the Al block. Thermocouples T₂-T₄ were positioned together elsewhere.

3.5 Characterization

3.5.1 Descriptive Results

A typical PuO₂ sample from an early batch (with a 30-mL crucible) is shown in Figure 3-2.



Figure 3-2. Typical PuO₂ Sample after Calcination

Samples from most batches were submitted for morphology characterization by SEM. Typical results for a PuO_2 and a Pu oxalate sample are shown in Figures 3-3 and 3-4, respectively. Additional examples are available in the pertinent laboratory notebook.¹³

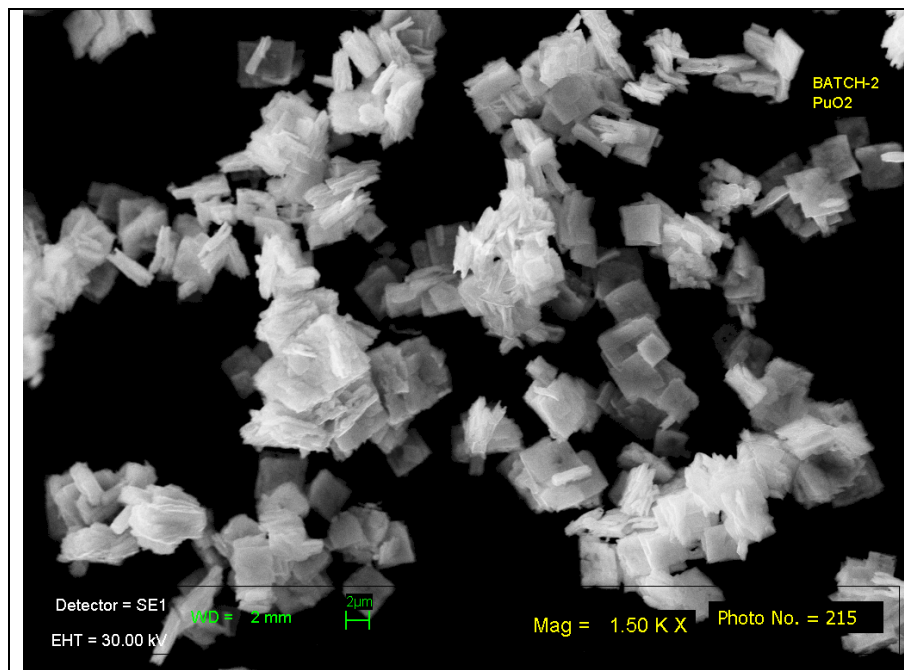


Figure 3-3. Typical SEM Results for PuO_2

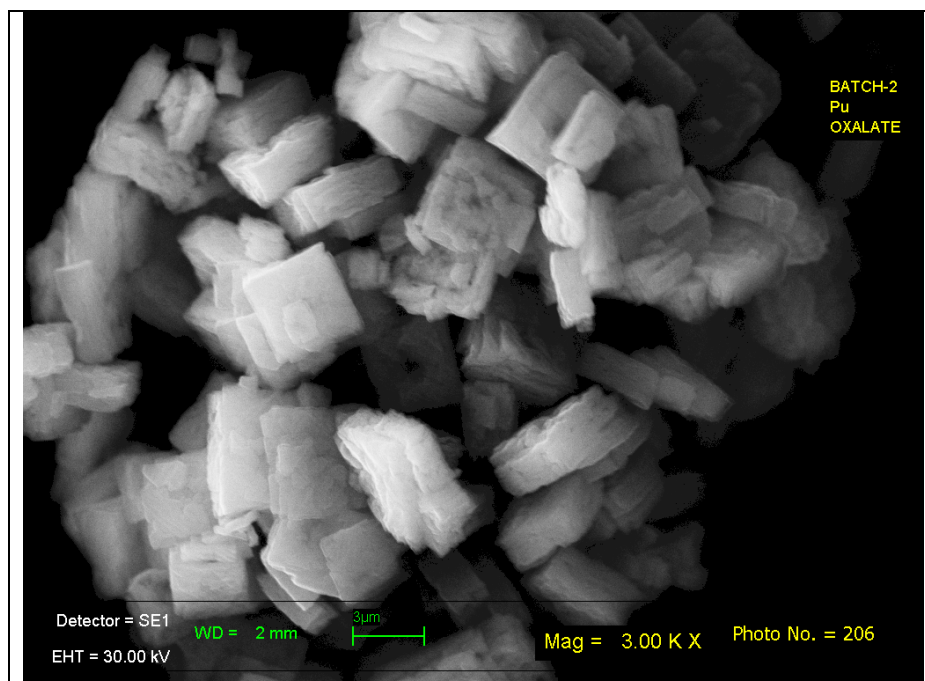


Figure 3-4. Typical SEM Results for Pu Oxalate

3.5.2 Moisture Analysis by TGA-MS

Typical TGA-MS plots for PuO_2 samples produced in this study are shown in Figures 3-5 through 3-7.

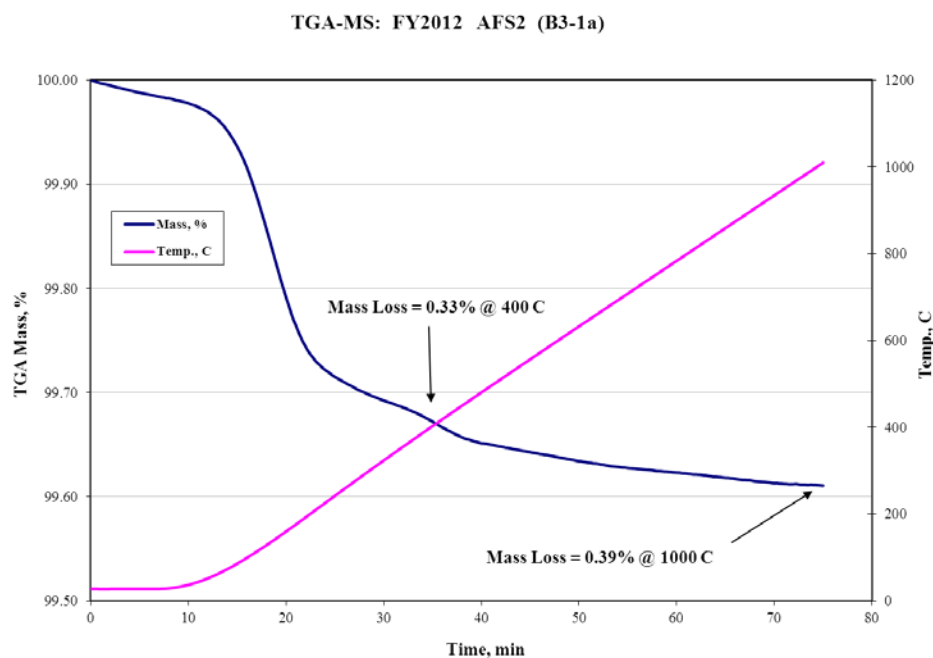


Figure 3-5. TGA Mass Measurement for Sample B3-1a

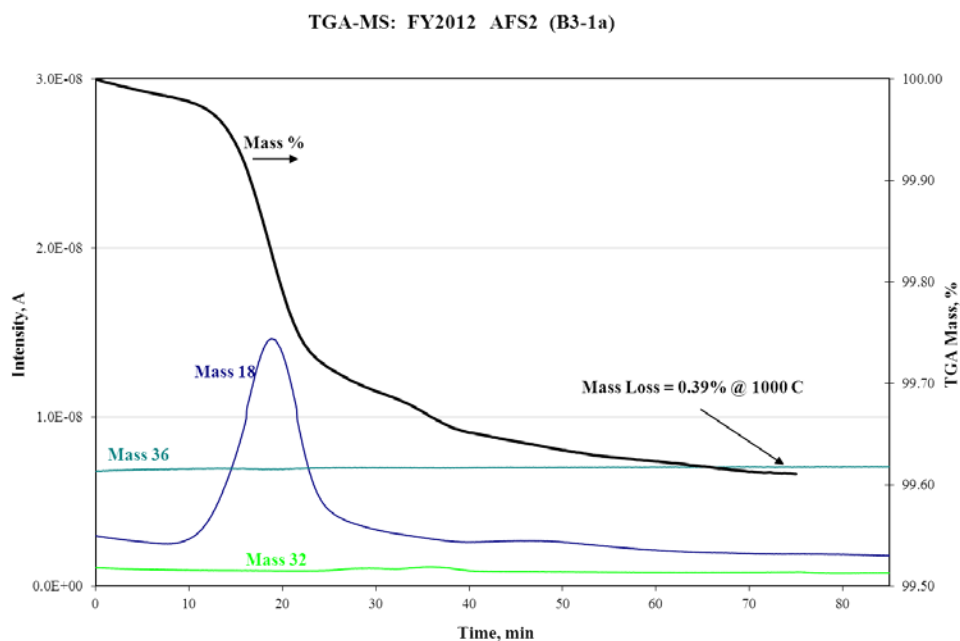


Figure 3-6. MS Signals (linear scale) from TGA-MS Analysis of Sample B3-1a

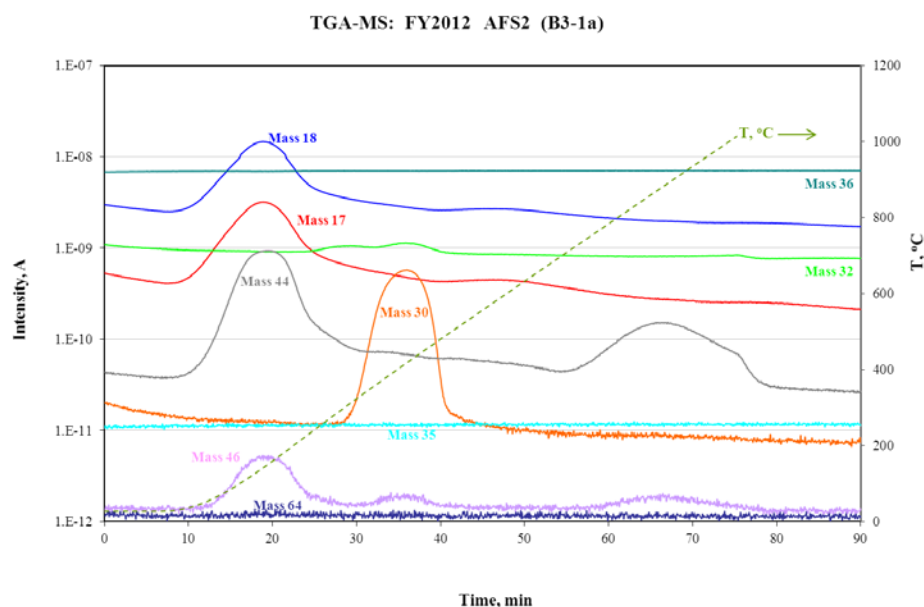


Figure 3-7. MS Signals (logarithmic scale) from TGA-MS Analysis of Sample B3-1a

As shown in Figures 3-5 through 3-7, heating to 400 °C caused release of nearly all of the moisture from Sample B3-1a. In addition, the largest portion of the carbon release, measured as Mass 44 or CO₂ (carbon dioxide), occurred in the same ~40-300 °C temperature range as the bulk of the moisture release. With carbon, however, the release of CO₂ continued through heating, with a second, smaller release centered at ~850 °C. A release of Mass 30, attributed to NO (nitric oxide), occurred in the 300 – 500 °C range. The MS showed no other significant gas releases, including no Mass 28, which can be attributed to CO (carbon monoxide).

For samples in this study, the general shape of the TGA-MS time/temperature profile of gases released did not change. As an example, TGA-MS results from another sample are shown in Figures 3-8 and 3-9. The TGA-MS results for a third sample are provided in the Appendix, and results from all the samples in this study are in the pertinent laboratory notebook.¹³ Table A-3 in the Appendix also provides 95% confidence limits for each of the MS moisture results, as calculated by JMP 5.0.1a statistical software and confirmed by Excel calculations. The confidence limits are based on the linearity of the pertinent moisture calibration curve generated by analysis of gypsum standards. Except for Batch 2 samples, the 95% confidence limits for MS moisture contents were $\pm 10\%$ of the reported value. Batch 2 values had higher uncertainties because one Batch 2 measurement involved a 3.7 g sample, which is well above typical amounts. To bound the moisture content of the larger sample, a large gypsum standard was required and thus a large crucible was required, which yields higher uncertainties. The testing of samples significantly greater than 3 g is not expected in future analyses.

Calibration of the TGA-MS for moisture using gypsum (CaSO₄•2H₂O) standards yielded moisture contents for each sample, which included in the summary Tables 3-7 and 3-8. The 95% Confidence Intervals for the MS moisture content values are provided in Appendix A. In a similar fashion, the 95% Confidence Intervals for the SSA values in Tables 3-7 and 3-8 are provided in Appendix A. Generally, SSA samples are analyzed in duplicate and the average is

reported. The confidence interval for a specific sample depends in part on the precision of the duplicate portions of that sample. For this study, the SSA 95% confidence intervals correspond to percentage uncertainties ranging from ± 1.5 to ± 4 .

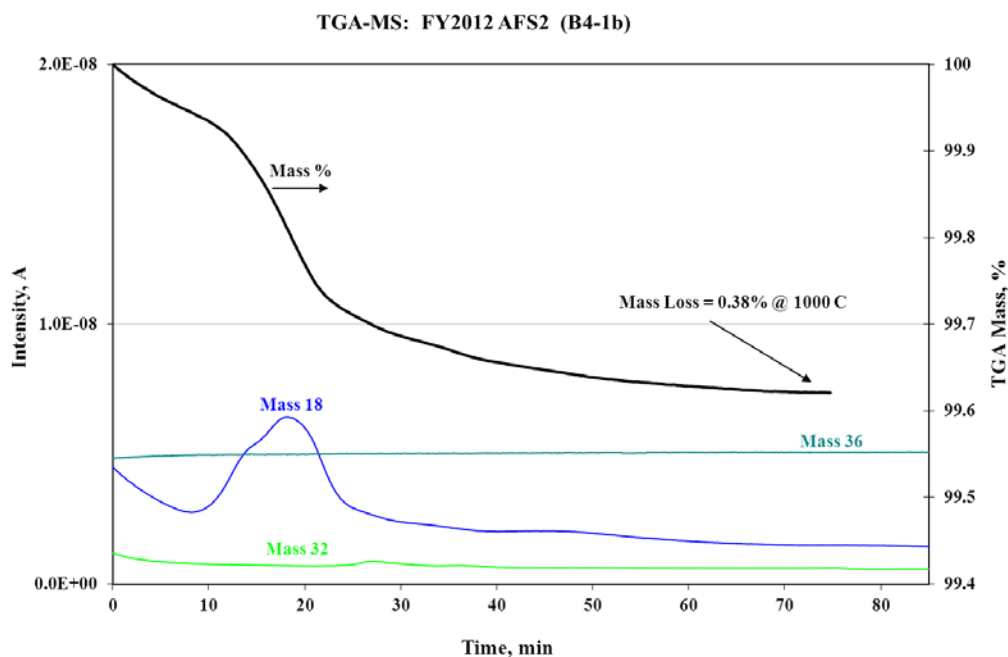


Figure 3-8. MS Signals (linear scale) from TGA-MS Analysis of Sample B4-1b

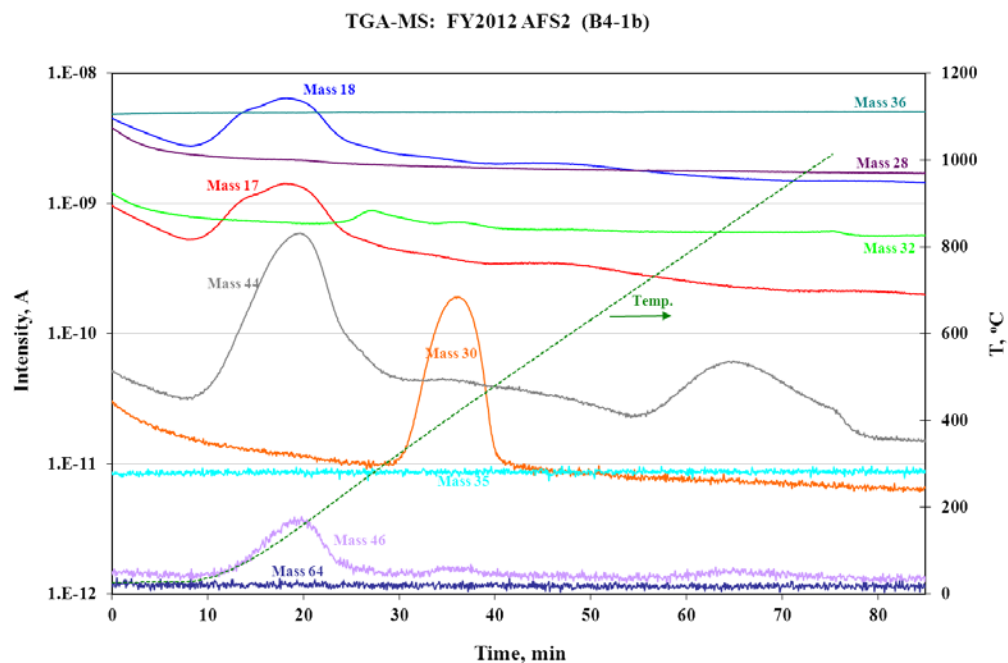


Figure 3-9. MS Signals (logarithmic scale) from TGA-MS Analysis of Sample B4-1b.

3.5.3 Carbon Analysis

Results for carbon content for the samples analyzed are shown in Table 3-7. A later report will compare carbon analysis by TGA-MS to these values measured by a carbon analyzer. The values in Table 3-7 show that the carbon contents of PuO₂ produced at SRNL easily met the Column A limit of 1000 µg C/g Pu, and the Column B limit of 500 µg C/g Pu, although the B4-1 sample would slightly exceed the Column B limit with the addition of ±10% uncertainty. For this carbon analysis, method development is not complete, but an uncertainty of ±10% is expected. The values in Table 3-7 reflect averages of duplicate analyses, and the duplicate results stayed within ±10% except where noted.

Table 3-7. Carbon Contents of PuO₂ Samples

Batch	C wt%	C µg/g sample	C µg/g Pu [†]
B3-5A	0.034	340	390
B3-5B	0.027	270	310
B4-1	0.042	420	480
B4-2	0.017	170	190
D5-A	0.023	230	260
D5-B	0.018	180	210
D30-A	0.023*	230	260
D30-B	0.020	200	220
D15-A	0.024	240	270
D15-B	0.029 [#]	290	330

* Result at ± 35%. [#] Result at ± 20%.

[†] Based on estimated assay of 0.87 g Pu/g PuO₂ sample.

3.5.4 Characterization Highlights

Tables 3-8 and 3-9 summarize TGA-MS and SSA results based on the processing conditions used during precipitation and calcination.

Table 3-8. Characterization Highlights of Calcination Batches 1-3

Sample ID	Calc. Temp. °C	Calc. Time, h	Specific Surface Area, m ² /g	Additional exposure time, h	RH [§] during exposure, %	TGA Mass loss to 1000 C, wt %	Moisture by MS wt %	Acidity of precipitator feed, M	Crucible holder? Y or N	Sample size, mg	Furnace Temp., °C
B1-2	~620*	2	13.5	---	---	0.58	0.42	0.77	N	1981	677
B1-3a	~650*	3	13.2	---	---	0.30	0.22	0.77	N	1414	
B1-3b	~650*	3		21	18.5	0.56	0.40	0.77	N	1290	
B1-4	~690*†	3	9.42	---	---	0.21	0.15	0.77	N	2021	
B1-5	~685*	3.7	9.09	---	---	0.24	0.18	0.77	N	2602	
B2-2a	610	2	14.1	---	---	0.55	0.45	0.77	N	1530	640
B2-2b	610	2		3	33.5	0.67	0.58	0.77	N	2313	
B2-3a	625	3	13.7	---	---	0.53	0.44	0.77	N	2235	640
B2-3b	625	3		18	33.5	0.79	0.66	0.77	N	2538	
B2-4	625	4	12.4	---	---	Inst. error	0.26	0.77	N	3599	650
B2-5	628	5	11.4	16	24.0	Inst. error	0.49	0.77	N	3654	650
B3-1a	650	4	7.83	---	---	0.39	0.32	0.77	N	1386	665
B3-1b	650	4		3	21.0	0.39	0.35	0.77	N	1794	
B3-2a	650	2	7.78	---	---	0.46	0.38	0.77	N	1262	666
B3-2b	650	2		4	33.1	0.49	0.42	0.77	N	1107	
B3-3a	650	3	5.61	---	---	0.34	0.30	0.77	N	1496	678
B3-3b	650	3		22	32.5	0.35	0.35	0.77	N	1069	
B3-4a	650	4	8.72	---	---	0.43	0.37	0.77	N	1282	656
B3-4b	650	4		3.5	29.4	0.43	0.36	0.77	N	962	
B3-5Aa	640	4	6.79	---	---	0.30	0.27	0.77	Y	1020	670
B3-5Ab	640	4		3	33.8	0.31	0.26	0.77	Y	881	
B3-5Ba	636	4	7.27	---	---	0.29	0.26	0.77	Y	1091	670
B3-5Bb	636	4		3	35.2	0.35	0.31	0.77	Y	922	

*Thermocouple not in contact with sample during calcination.

†Plus an additional 0.7 hours at ~655 °C*.

§ RH values may be biased low by 5-10 units based on newly calibrated humidity meter.

Table 3-9. Characterization Highlights of Additional Calcination Batches

Sample ID	Calc. Temp. °C	Calc. Time, h	Specific Surface Area, m ² /g	Additional exposure time, h	RH [§] during exposure, %	TGA Mass loss to 1000 C, wt %	Moisture by MS wt %	Acidity of precipitator feed, M	Digestion time min	Sample size, mg	Furnace Temp., °C
B4-1a	635	4	6.87	---	---	0.29	0.26	2.5-3.0	6	761	658
B4-1b	635	4		4	35.1	0.38	0.34	2.5-3.0	6	1208	
B4-2a	650	4	5.20	---	---	0.26	0.20	2.5-3.0	6	538	658
B4-2b	650	4		3	17	0.30	0.21	2.5-3.0	6	593	
B4-2c	650	4		19.5	21	0.30	0.22	2.5-3.0	6	509	
D5-A	617	4	8.13	---	---	0.49	0.38	1.23-1.5*	5	559	656-670
D5-B	650	4	7.49	---	---	0.42	0.31	1.23-1.5*	5	448	656-670
D5-Bb				3	34.0 - 35.8	0.46	0.30			242	
D30-A	650	4	5.33	---	---	0.32	0.23	1.23-1.5*	30	586	695
D30-B	636	4	8.98	---	---	0.46	0.35	1.23-1.5*	30	418	671-679
D30-Bb				3	39.0-39.0	0.55	0.43			508	
D15-A	650	4	7.15	---	---	0.42	0.34	1.23-1.5*	15	607	684-699
D15-Ab				66	36.1 - 18.0	0.44	0.30			455	
D15-B	635	4	9.71	---	---	0.44	0.33	1.23-1.5*	15	749	676-702
D15-Bb				16	15.7 - 16.8	0.53	0.40			632	

Note: All samples on this page were calcined in a quartz crucible setting inside a firebrick crucible holder.

*Free acid analyses of a precipitator feed samples report 1.23 and 1.33 M. Volume additions indicated an acid concentration of 1.5 M.

§ RH values may be biased low by 5-10 units based on newly calibrated humidity meter.

3.5.5 Particle Size Analysis

Additionally, personnel performed particle size analysis on both PuO₂ and Pu oxalate samples. The results are summarized in Tables 3-10 and 3-11 and the plots of particle size distribution are provided in Appendix C.

Table 3-10. Particle Size Analyses of PuO₂ Samples

Sample ID	Particle Size Range μm	Mean* Particle Size μm	Standard Deviation μm
Batch 1 PuO ₂	0.204 – 62.23	6.647	3.557
Batch 2 PuO ₂	NM	NM	NM
Batch 3 PuO ₂	0.204 – 44.00	6.365	3.981
Batch 4 PuO ₂	0.204 – 74.00	9.255	6.168
Batch D-5A PuO ₂	0.204 – 88.00	8.758	5.808
Batch D-5B PuO ₂	0.204 – 88.00	9.273	5.976
Batch D-30 PuO ₂	0.204 – 62.23	6.662	3.630
Batch D-15 PuO ₂	0.204 – 88.00	8.295	5.016

*Mean Particle Size determined on a volumetric basis.

NM – Not Measured

Table 3-11. Particle Size Analyses of Pu Oxalate Samples

Sample ID	Particle Size Range μm	Mean* Particle Size μm	Standard Deviation μm	Comments
Batch 2 Pu Oxalate	0.172 – 352.0	23.91	17.98	Bi-modal distribution
Batch 4 Pu Oxalate	0.172 – 124.5	16.18	11.25	Bi-modal distribution
Batch D-5 Pu Oxalate	0.344 – 124.5	13.10	7.949	---
Batch D-30 Pu Oxalate	0.172 – 88.00	10.54	6.349	---
Batch D-15 Pu Oxalate	0.344 – 124.5	13.20	7.566	---

*Mean Particle Size determined on a volumetric basis.

3.6 Review of Moisture Analyses

Extracting key information from Tables 3-8 and 3-9 allows the comparisons in Table 3-12. One observation from the calculated ratio of MS moisture/TGA mass loss is that the MS moisture content averages $80 \pm 8\%$ of the total TGA mass loss. Similarly, these samples consistently showed nominally 2 monolayer equivalents of moisture, using the accepted value of 0.22 mg H₂O/m² per monolayer¹⁴.

Table 3-12. Relations Between MS Moisture, TGA, and SSA

Batch	SSA m²/g	MS wt%	MS/ TGA	H₂O mg/m²	Monolayer equiv.
B1-2	13.5	0.42	0.72	0.31	1.4
B1-3a	13.2	0.22	0.73	0.17	0.8
B1-3b	13.2	0.40	0.71	0.30	1.4
B1-4	9.42	0.15	0.71	0.16	0.7
B1-5	9.09	0.18	0.75	0.20	0.9
B2-2a	14.1	0.45	0.82	0.32	1.5
B2-2b	14.1	0.58	0.87	0.41	1.9
B2-3a	13.7	0.44	0.83	0.32	1.5
B2-3b	13.7	0.66	0.84	0.48	2.2
B2-4	12.4	0.26	NA	0.21	1.0
B2-5	11.4	0.49	NA	0.43	2.0
B3-1a	7.83	0.32	0.82	0.41	1.9
B3-1b	7.83	0.35	0.90	0.45	2.0
B3-2a	7.78	0.38	0.83	0.49	2.2
B3-2b	7.78	0.42	0.86	0.54	2.5
B3-3a	5.61	0.30	0.88	0.53	2.4
B3-3b	5.61	0.35	1.00	0.62	2.8
B3-4a	8.72	0.37	0.86	0.42	1.9
B3-4b	8.72	0.36	0.84	0.41	1.9
B3-5Aa	6.79	0.27	0.90	0.40	1.8
B3-5Ab	6.79	0.26	0.84	0.38	1.7
B3-5Ba	7.27	0.26	0.90	0.36	1.6
B3-5Bb	7.27	0.31	0.89	0.43	1.9
B4-1a	6.87	0.26	0.90	0.38	1.7
B4-1b	6.87	0.34	0.89	0.49	2.2
B4-2a	5.20	0.20	0.77	0.38	1.7
B4-2b	5.20	0.21	0.70	0.40	1.8
B4-2c	5.20	0.22	0.73	0.42	1.9
D5-A	8.13	0.38	0.78	0.47	2.1
D5-B	7.49	0.31	0.74	0.41	1.9
D5-Bb	7.49	0.30	0.65	0.40	1.8
D30-A	5.33	0.23	0.72	0.43	2.0
D30-B	8.98	0.35	0.76	0.39	1.8
D30-Bb	8.98	0.43	0.78	0.48	2.2
D15-A	7.15	0.34	0.81	0.48	2.2
D15-Ab	7.15	0.30	0.68	0.42	1.9
D15-B	9.71	0.33	0.75	0.34	1.5
D15-Bb	9.71	0.40	0.75	0.41	1.9
		Average	0.80	Average without Batch 1	1.8
		Std. Dev.	0.08	Std. Dev.	0.33

NA = Not available due to TGA instrument error.

3.7 Statistical Analyses

The calcination data of plutonium oxalate ($\text{Pu}(\text{C}_2\text{O}_4)_2$) into PuO_2 was analyzed with JMP 5.0.1a looking at the effect of calcination temperature, calcination time, batch size, digestion time, and initial precipitation feed acidity on the SSA of the PuO_2 . After performing leverage analyses of the data in Table 3-13, two cases of interest are reported. For Case 1, all the data was included but Feed Acidity was not a potential factor. In Case 2, Feed Acidity was included as a potential factor. For Case 2, the software tested for effects with all of the data and with Batch 1 data excluded, since the temperatures reported for Batch 1 have higher uncertainties.

Table 3-13. Summary of Data for Statistical Analysis

Batch	Sample	SSA, m^2/g	Calc. Temp. $[\text{°C}]$	Calc. Time [h]	Batch size [g]	Digestion Time [h]	Feed Acidity [M]
1	B1-2	13.5	620	2	3.01	0.283	0.77
1	B1-3	13.2	650	3	4.14	0.283	0.77
1	B1-4	9.42	690	3	2.98	0.283	0.77
1	B1-5	9.09	685	3.7	3.64	0.283	0.77
2	B2-2	14.1	610	2	4.67	0.217	0.77
2	B2-3	13.7	625	3	5.65	0.217	0.77
2	B2-4	12.4	625	4	4.41	0.217	0.77
2	B2-5	11.4	628	5	4.49	0.217	0.77
3	B3-1	7.83	650	4	4.1	0.25	0.77
3	B3-2	7.78	650	2	3.33	0.25	0.77
3	B3-3	5.61	650	3	4.08	0.25	0.77
3	B3-4	8.72	650	4	3.39	0.25	0.77
3	B3-5A	6.79	640	4	3.33	0.25	0.77
3	B3-5B	7.27	636	4	3.36	0.25	0.77
4	B4-1	6.87	635	4	3.5	0.10	3.0
4	B4-2	5.20	650	4	3.36	0.10	3.0
D5	D5-A	8.13	617	4	2.09	0.083	1.28
D5	D5-B	7.49	650	4	2.34	0.083	1.28
D30	D30-A	5.33	650	4	2.01	0.5	1.28
D30	D30-B	8.98	636	4	2.63	0.5	1.28
D15	D15-A	7.15	650	4	2.56	0.25	1.28
D15	D15-B	9.71	635	4	2.64	0.25	1.28

The JMP statistical software developed a model and a corresponding fit of actual SSA results versus SSA values predicted by the model. For Case 1, the RSquare value in the Summary of Fit, shown in Table 3-14, indicates that some dependence of SSA is captured by the various effects (e.g., calcination temp.). Then, the Parameter Estimate, shown in Table 3-15, provides t-statistic values, which indicate that Batch Size (g) is a significant or non-zero effect and has a more significant effect than Calcination Temp. (°C) and Calcination Time (h), which may be interacting with Batch Size. Also, Digestion Time (h) is not a significant effect. These results are indicated in Table 3-15 where the probability that the parameter estimate is zero ($\text{prob}>|t|$) is about 2% for the Batch Size, 9% for the Calcination Temp., 12% for the Calc. Time and 43% for the Digestion Time. The Summary of Fit, shown in Table 3-14, indicates that the SSA is not a simple linear function of the calcination temperature, time, and batch size by the adjusted R^2 of only 0.39. The prior literature review⁶ of PuO_2 SSA data indicated that calcination temperature and time were primary effects on SSA and that the dependence was not linear.

Table 3-14. Statistical Summary of Fit – Case 1: All Data, 4 Parameters

RSquare	0.5091
RSquare Adj	0.3936
Root Mean Square Error	2.1833
Mean of Response	9.076
Observations (or Sum Wgts)	22

Table 3-15. Statistical Parameter Estimate– Case 1: All Data, 4 Parameters

Term	Estimate	Std Error	t Ratio	Prob> t
Intercept	36.81	16.98	2.17	0.0446
Calc. Temp. [°C]	-0.0464	0.0257	-1.81	0.0887
Calc. Time [h]	-1.010	0.6231	-1.62	0.1233
Batch Size [g]	1.391	0.5561	2.50	0.0229
Digestion Time [h]	3.749	4.678	0.80	0.4339

For Case 2, the statistical results showed that both Calcination Temperature and Batch Size have a significant effect on the SSA but that the other parameters do not. Since the Case 2 results which excluded Batch 1 data had a better fit, those results are reported in Tables 3-16 and 3-17. From Table 3-17, the probability that the parameter estimate is zero (prob>|t|) is about 0.2% for the Calcination Temp., 4% for the Batch Size, 20% for the Feed Acidity, and significantly higher (less likely to have an effect) for Digestion Time and Calcination Time.

Table 3-16. Statistical Summary of Fit – Case 2: Omit Batch 1 Data, 5 Parameters

RSquare*	0.7844
RSquare Adj	0.6946
Root Mean Square Error	1.4923
Mean of Response	8.5811
Observations (or Sum Wgts)	18

*RSquare indicates that excluding Batch 1 data gives a better fit to SSA than including Batch 1, and a better fit than Case 1.

Table 3-17. Statistical Parameter Estimate– Case 2: Omit Batch 1 Data, 5 Parameters

Term	Estimate	Std Error	t Ratio	Prob> t
Intercept	85.17	20.0565	4.25	0.0011
Calc. Temp. [°C]	-0.1245	0.03078	-4.05	0.0016
Calc. Time [h]	0.00530	0.5147	0.01	0.9920
Batch Size [g]	1.0267	0.4339	2.37	0.0356
Digestion Time [h]	1.281	3.553	0.36	0.7248
Feed Acidity [M]	-0.8115	0.6013	-1.35	0.2021

Excluding Batch 1 data indicates that Calc. Temp. [°C] and Batch Size [g] are significant or non-zero effects and Calc. Time [h], Digestion Time [h], and Feed Acidity [M] are not significant effects. Including Batch 1 data yielded the same results as to which parameters are significant effects on SSA.

Though the statistical analyses showed that Batch Size had a significant effect on SSA in this study, the actual range of Batch Sizes tested, 2.01 – 5.65 g PuO₂, seems too narrow for a Batch Size evaluation. A study planned to follow this study will have two PuO₂ batch sizes of ~40 g, which may help in evaluating this factor. In addition, historical experience with neptunium oxide (NpO₂) production in HB-line showed similar SSA values between SRNL-produced NpO₂ on the 25-g scale and HB-Line NpO₂ produced on the 1-kg scale,² where calcination temperatures and times were also similar.

4.0 Conclusions

An anion exchange column experiment produced 1.4 L of a purified 52.6 g/L Pu solution. Over the next nine weeks, seven Pu(IV) oxalate precipitations were performed using the same stock Pu solution, with precipitator feed acidities ranging from 0.77 M to 3.0 M nitric acid and digestion times ranging from 5 to 30 minutes. Analysis of precipitator filtrate solutions showed Pu losses below 1% for all precipitations. The four larger precipitation batches matched the target oxalic acid addition time of 44 minutes within 4 minutes. For the three smaller precipitation batches that focused on evaluation of digestion time, the oxalic acid addition step ranged from 25-34 minutes because of pump limitations in the low flow range.

Following the precipitations, 22 calcinations were performed in the range of 610 – 690 °C, with the largest number of samples calcined at 650 or 635 °C. Characterization of the resulting PuO₂ batches showed specific surface areas in the range of 5-14 m²/g, with 16 of the 22 samples in the range of 5-10 m²/g. For samples analyzed with typical handling (exposed to ambient air for 15-45 minutes with relative humidities of 20-55%), the moisture content as measured by MS ranged from 0.15 to 0.45 wt % and the total mass loss at 1000 °C, as measured by TGA, ranged from 0.21 to 0.58 wt %. For the samples calcined between 635 and 650 °C, the moisture content without extended exposure ranged from 0.20 to 0.38 wt %, and the TGA mass loss ranged from 0.26 to 0.46 wt %. Of these latter samples, the samples calcined at 650 °C generally had lower specific surface areas and lower moisture contents than the samples calcined at 635 °C, which matches expectations from the literature.

Taken together, the TGA-MS results for samples handled at nominally 20-50% RH, without extended exposure, indicate that the Pu(IV) oxalate precipitation process followed by calcination at 635-650 °C appears capable of producing PuO₂ with moisture content < 0.5 wt % as required by the 3013 Standard.

Exposures of PuO₂ samples to ambient air for 3 or more hours generally showed modest mass gains that were primarily gains in moisture content. These results point to the need for a better understanding of the moisture absorption of PuO₂ and serve as a warning that extended exposure times, particularly above the 50% RH level observed in this study will make the production of PuO₂ with less than 0.5 wt % moisture more challenging. Samples analyzed in this study generally contained approximately 2 monolayer equivalents of moisture.

In this study, the bulk of the moisture released from samples by 300 °C, as did a significant portion of the CO₂. Samples in this study consistently released a minor amount of NO in the ~40-300 °C range, but no samples released CO or SO₂. TGA-MS results also showed that MS moisture content accounted for 80±8% of the total mass loss at 1000 °C measured by the TGA.

The PuO₂ samples produced had particles sizes that typically ranged from 0.2 – 88 µm, with the mean particle size ranging from 6.4 – 9.3 µm. The carbon content of ten different calcination batches ranged from 190-480 µg C/g Pu, with an average value of 290 µg C/g Pu.

A statistical review of the calcination conditions and resulting SSA values showed that in both cases tested, calcination temperature had a significant effect on SSA, as expected from literature data. The statistical review also showed that batch size had a significant effect on SSA, but the narrow range of batch sizes tested is a compelling reason to set aside that result until tests with larger batch sizes are completed. When feed acidity was not included as a variable, calcination time had a significant effect on SSA. However, including feed acidity as a variable showed that neither feed acidity nor calcination time had a significant effect on SSA in this study. Also, for both cases the statistical review also indicated that digestion time did not have a significant effect on SSA.

5.0 Recommendations

Complete the two larger (~40 g) batch syntheses of PuO₂ as planned to investigate the impacts on properties. Examine moisture sorption behavior of that material under a broader range of relative humidity values, to include humidities representative of the HB-Line facility. In addition, SRNL recommends that the range of acceptable precipitator acidities be re-considered, as acidities below 1.5 M in this study did not show significant Pu losses, and showed similar SSA values at the same calcination conditions as materials precipitated at higher acidities.

6.0 References

- ¹ Christopher, J.W., Task Technical Request, “Flow Sheet Verification for HB-Line Phase II Plutonium Oxide Production PPT/FLT/Calcination Operations and 3013 Equivalency”, NMMD-HTS-2011-3178, November 22, 2011.
- ² Crowder, M.L., and J.M. Duffey, “Task Technical and Quality Assurance Plan for Precipitation and Calcination of Plutonium(IV) Oxalate to Form Plutonium Oxide and Subsequent Gas Generation Studies to Support the MOX Feed Mission”, SRNL-RP-2011-01657, Rev. 0, January 15, 2011.
- ³ Smith, R.H., “HB-Line Pu-239 Production Flow Sheet Strategy (U)”, SRNS-E1100-2011-00025, October 12, 2011.
- ⁴ *Stabilization, Packaging, and Storage of Plutonium-bearing Materials*. 2004. DOE-STD-3013-2004. U.S. Department of Energy: Washington, D.C.
- ⁵ Bluhm, E.A., et al, “Plutonium Oxide Polishing for MOX Fuel Production”, *Separation Science and Technology*, 40:281-296, 2005.
- ⁶ Daniel, W.E., “Literature Review of PuO₂ Calcination Time and Temperature Data for Specific Surface Area”, SRNL-TR-2011-00334, Rev. 0, March 6, 2012.
- ⁷ Rudisill, T.S., and R.A. Pierce, “Dissolution of Pu Metal in 8-10 M Nitric Acid” SRNL-STI-2012-00043, Rev. 0, February 2012.
- ⁸ Jones, M.A., D.P. DiPrete, B.J. Wiedenman, “Application of Column Extraction Method for Impurities Analysis on HB-Line Plutonium Oxide in Support of MOX Feed Product Specifications”, SRNL-STI-2012-00148, Rev. 0, March 2012.
- ⁹ Bronikowski, M.G., J.M. Duffey, and R.R. Livingston, “Lab Scale Production of NpO₂”, WSRC-TR-2003-00392, August 2003.
- ¹⁰ Duffey, J.M., B.C. Hill, and R.R. Livingston, “Capability for Moisture Removal from Neptunium Oxide by the HB-Line 9975 Inerting Process”, WSRC-TR-2004-00602, February 2005.
- ¹¹ Aluminum Construction Manual, 3rd Ed., Section 3 “Engineering Data for Aluminum Structures”, p. 6, The Aluminum Association, New York, January 1975.
- ¹² “Typical properties of aluminum wrought alloys”, Machine Design, Section 2 Nonferrous Metals, Penton Publishing, April 17, 1986.
- ¹³ Crowder, M L., “Actinide Processing III”, Laboratory Notebook SRNL-NB-2012-00010.
- ¹⁴ Haschke, J. M. and T.E. Ricketts, “Adsorption of water on plutonium dioxide”. *Journal of Alloys and Compounds* **1997**, 252, 148-156.

Appendix A

Table A-1. Anion Exchange Results for Pu and Am.

Sample	Volume (mL)	Gamma PHA Pu239 (dpm/mL)	Pu239 Gamma PHA (grams)	Total WG Pu (grams)	Gamma PHA Am241 (dpm/mL)	Am241 Gamma PHA (grams)
3013 DE Feed	4400	1.24E+09	39.6	42.1	2.46E+08	1.42E-01
Pu-B Feed	1550	6.33E+08	7.11	7.57	1.57E+08	3.67E-02
Pu-Gd Feed	1780	5.86E+08	7.56	8.05	1.50E+08	3.05E-02
Pu-Gd/B Feeds	2590	Analyzed previously		~17.1		
		Total Pu Fed		~74.8		
3013DE Eff	4000	<7.60E+05	<2.21E-02	<2.35E-02	5.34E+07	2.80E-01
Am Wash	1600	<6.89E+06	<8.00E-02	<8.52E-02	2.29E+08	4.81E-02
B Feed Eff	3500	<3.34E+06	<8.48E-02	<9.03E-02	1.41E+08	6.48E-02
Gd Feed Eff	2000	<3.90E+06	<5.66E-02	<6.03E-02	1.35E+08	3.55E-02
Gd Feed/Wash 1	3000	<4.00E+06	<8.70E-02	<9.27E-02	1.52E+08	5.99E-02
Wash 2	2000	3.39E+06	4.92E-02	5.24E-02	4.19E+07	1.10E-02
Wash 3	2000	1.97E+06	2.86E-02	3.05E-02	1.33E+07	3.49E-03
Wash 4	1750	<1.55E+06	<1.97E-02	<2.10E-02	3.13E+06	7.19E-04
Heads	1265	4.51E+06	4.14E-02	4.41E-02	2.75E+06	4.57E-04
Hearts	1400	6.82E+09	6.93E+01	7.38E+01	1.88E+07	3.46E-03
Tails 1	1000	6.78E+07	4.92E-01	5.24E-01	8.09E+04	1.06E-05
Tails 2	2000	1.67E+07	2.42E-01	2.58E-01	7.24E+04	1.90E-05

Table A-2. Impurity Content in Anion Exchange Feed by ICPES

Element	3013 DE Feed mg/L	Element	3013 DE Feed mg/L
Al	681	Li	0.675
B	3.05	Mg	103
Be	4.35	Mn	2.97
Ca	68.7	Mo	6.89
Cd	0.811	Na	27100
Ce	< 0.97	Ni	214
Co	< 0.85	Pb	< 7.16
Cr	103	S	< 12
Cu	30	Si	13.3
Fe	82.5	Ti	1.95
Gd	< 0.78	V	< 0.47
K	20.8	Zn	1.9

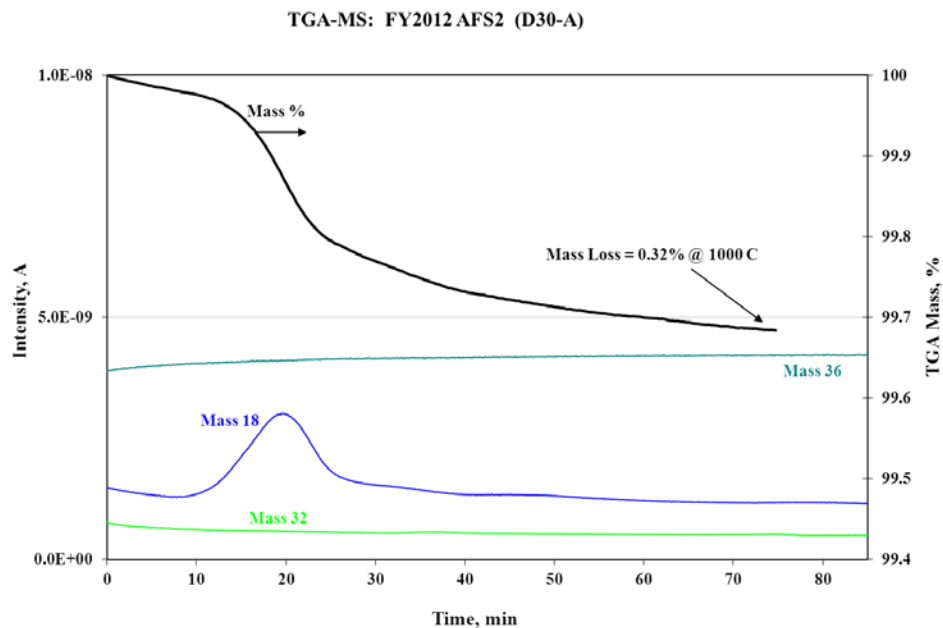


Figure A-1. MS Signals (linear scale) from TGA-MS Analysis of Sample D30-A.

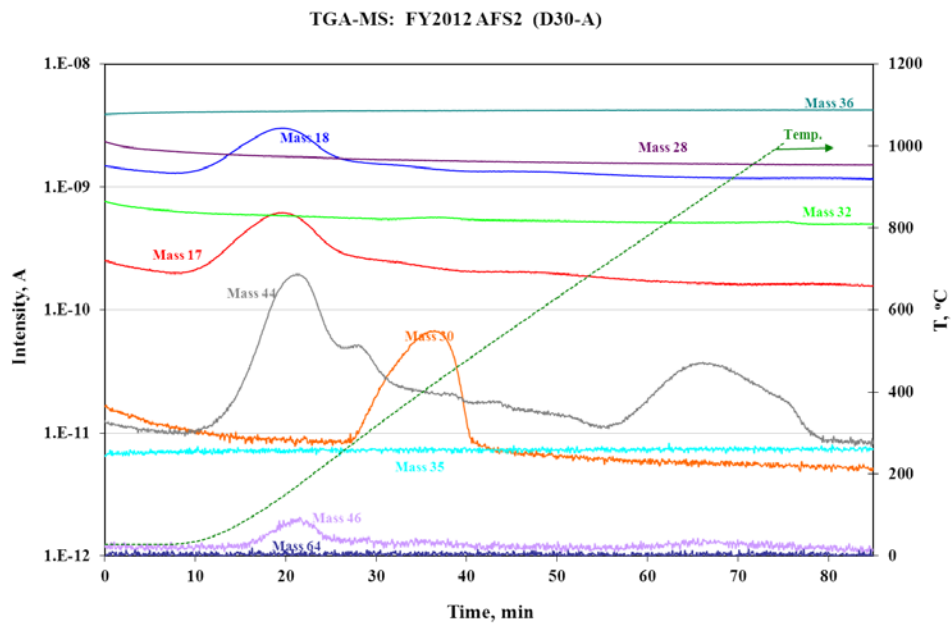


Figure A-2. MS Signals (logarithmic scale) from TGA-MS Analysis of Sample D30-A.

Table A-3. Uncertainties in MS Moisture Contents

Batch ID	MS Moisture Content, wt %	95% Confidence Interval	
		Lower Bound	Upper Bound
B1-2	0.42	0.40	0.44
B1-3a	0.22	0.21	0.23
B1-3b	0.40	0.39	0.43
B1-4	0.15	0.14	0.15
B1-5	0.18	0.17	0.19
B2-2a [†]	0.45	0.35	0.55
B2-2b [†]	0.58	0.51	0.65
B2-3a [†]	0.44	0.37	0.51
B2-3b [†]	0.66	0.59	0.73
B2-4 [†]	0.26	0.22	0.30
B2-5 [†]	0.49	0.44	0.54
B3-1a	0.32	0.31	0.34
B3-1b	0.35	0.33	0.37
B3-2a	0.38	0.37	0.40
B3-2b	0.42	0.40	0.45
B3-3a	0.30	0.29	0.32
B3-3b	0.35	0.33	0.37
B3-4a	0.37	0.35	0.39
B3-4b	0.36	0.34	0.38
B3-5Aa	0.27	0.26	0.29
B3-5Ab	0.26	0.25	0.28
B3-5Ba	0.26	0.24	0.27
B3-5Bb	0.31	0.30	0.33
B4-1a	0.26	0.25	0.27
B4-1b	0.34	0.32	0.36
B4-2a	0.20	0.19	0.21
B4-2b	0.21	0.20	0.22
B4-2c	0.22	0.21	0.23
D5-A	0.38	0.37	0.39
D5-B	0.31	0.30	0.32
D5-Bb	0.30	0.30	0.31
D30-A	0.23	0.23	0.24
D30-B	0.35	0.35	0.36
D30-Bb	0.43	0.42	0.44
D15-A	0.34	0.33	0.34
D15-Ab	0.30	0.29	0.31
D15-B	0.33	0.33	0.34
D15-Bb	0.40	0.39	0.41

[†] Range in 95% confidence limits greater than $\pm 10\%$ for these values because one large sample size (3.7 g) required a large gypsum standard amount tested in a large crucible that caused higher uncertainty.

Table A-4. Specific Surface Area Measurements with Uncertainties

Batch ID	SSA, m ² /g	95% Confidence Interval	
		Lower Bound	Upper Bound
B1-2	13.5	13.4	13.7
B1-3	13.2	13.1	13.4
B1-4	9.42	9.27	9.57
B1-5	9.09	8.93	9.24
B2-2	14.1	13.9	14.3
B2-3	13.7	13.5	13.9
B2-4	12.4	12.2	12.6
B2-5	11.4	11.2	11.5
B3-1	7.83	7.64	8.03
B3-2	7.78	7.58	7.97
B3-3	5.61	5.40	5.82
B3-4	8.72	8.53	8.92
B3-5A	6.79	6.60	6.97
B3-5B	7.27	7.07	7.47
B4-1	6.87	6.71	7.04
B4-2	5.20	5.00	5.41
D5-A	8.13	7.95	8.30
D5-B	7.49	7.30	7.68
D30-A	5.33	5.11	5.56
D30-B	8.98	8.78	9.19
D15-A	7.15	6.96	7.34
D15-B	9.71	9.51	9.92

Appendix B

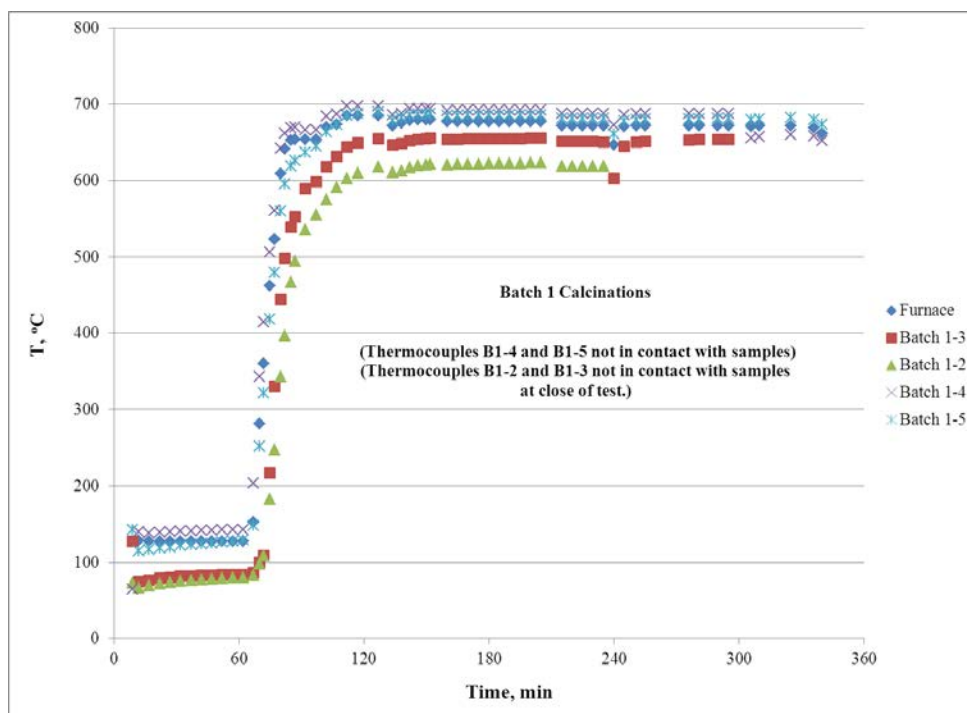


Figure B-1. Temperature Profiles for Batch 1 Calcinations

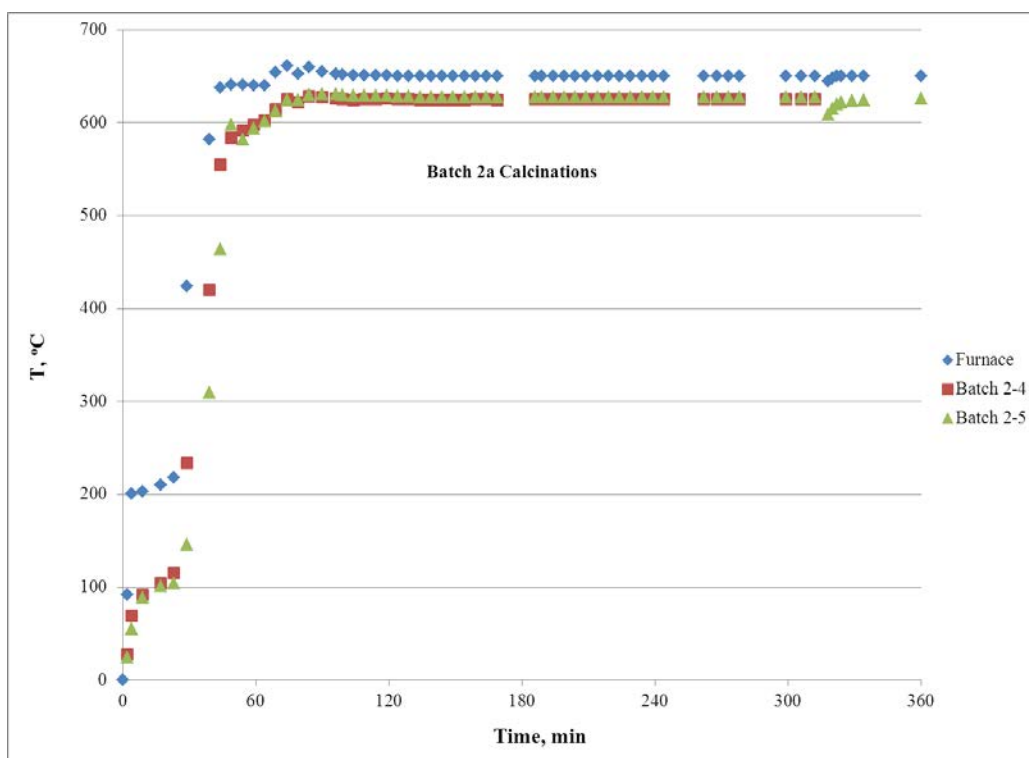


Figure B-2. Temperature Profiles for Batch 2a Calcinations

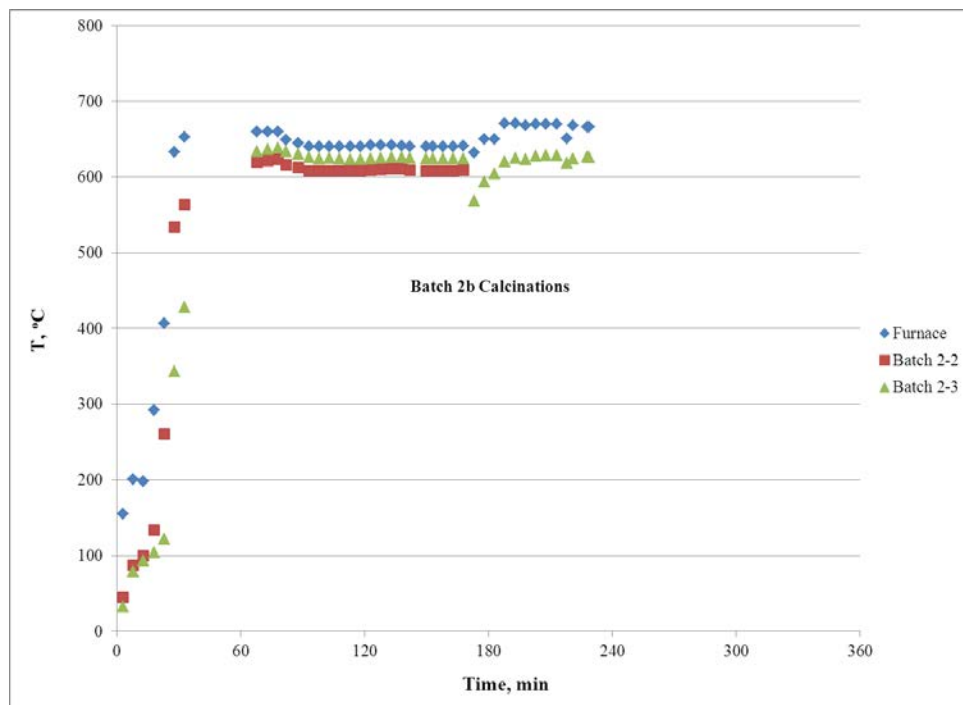


Figure B-3. Temperature Profiles for Batch 2b Calcinations

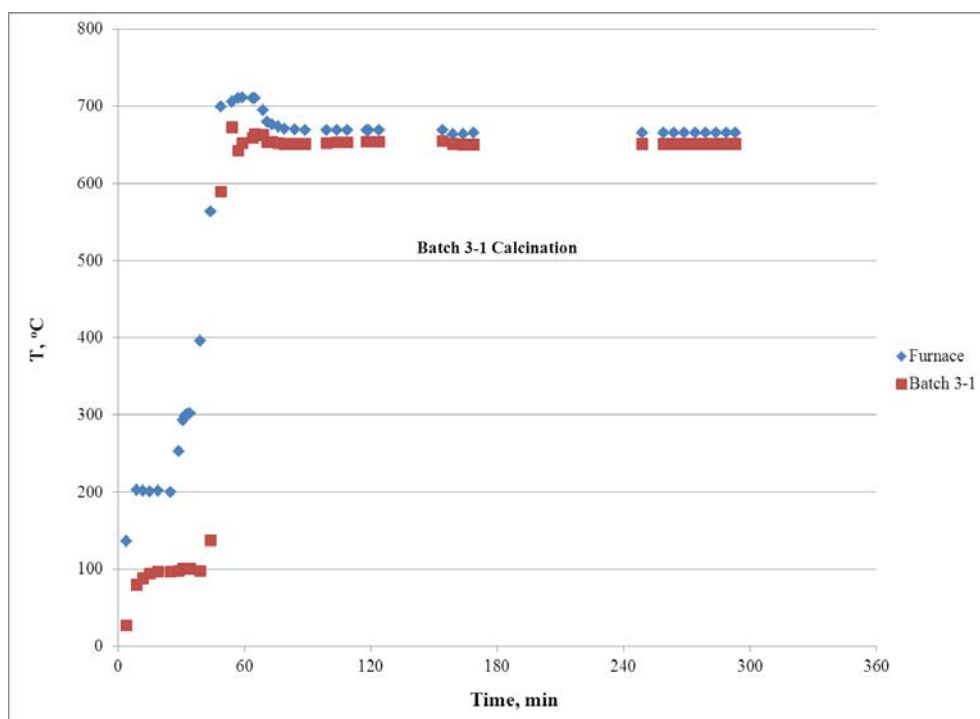


Figure B-4. Temperature Profile for Batch 3-1 Calcination

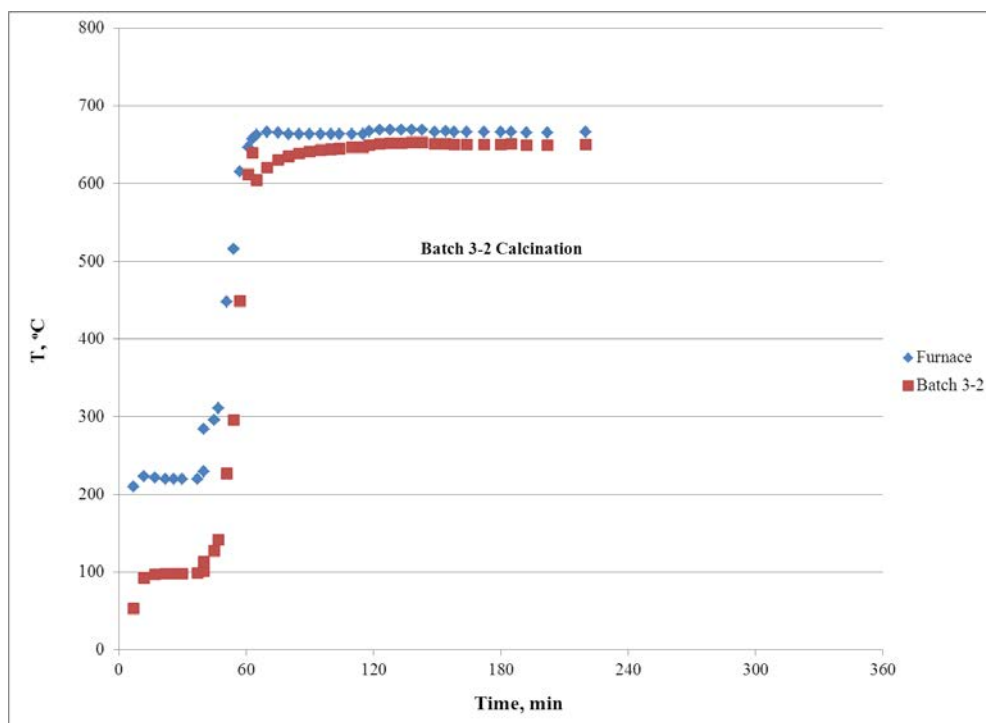


Figure B-5. Temperature Profile for Batch 3-2 Calcination

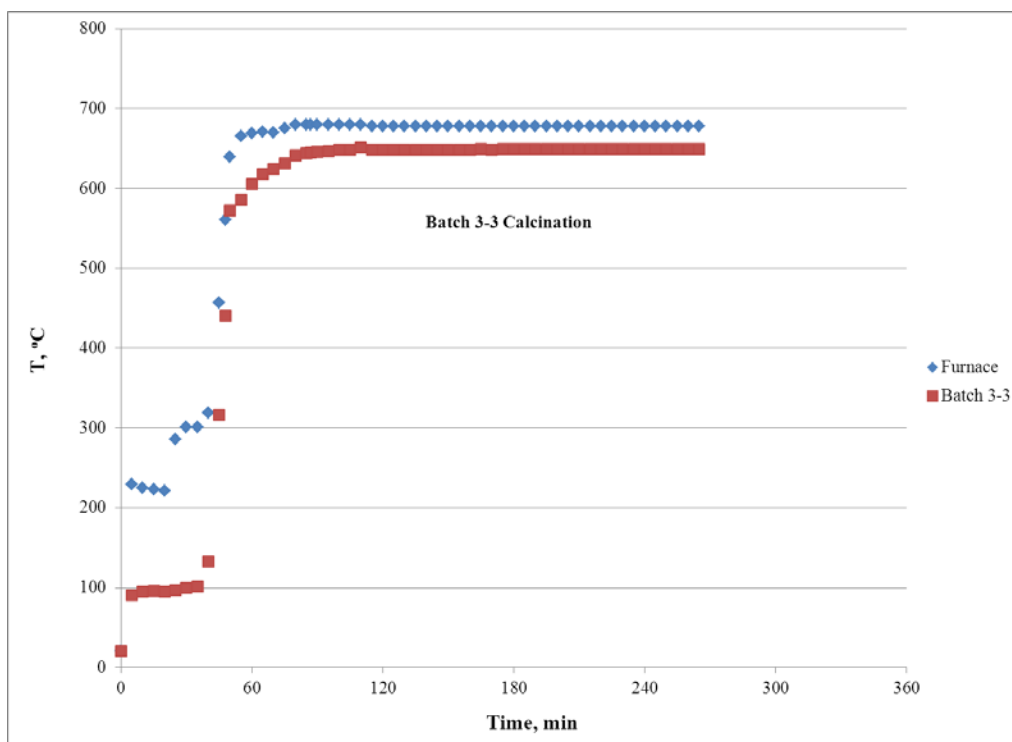


Figure B-6. Temperature Profile for Batch 3-3 Calcination

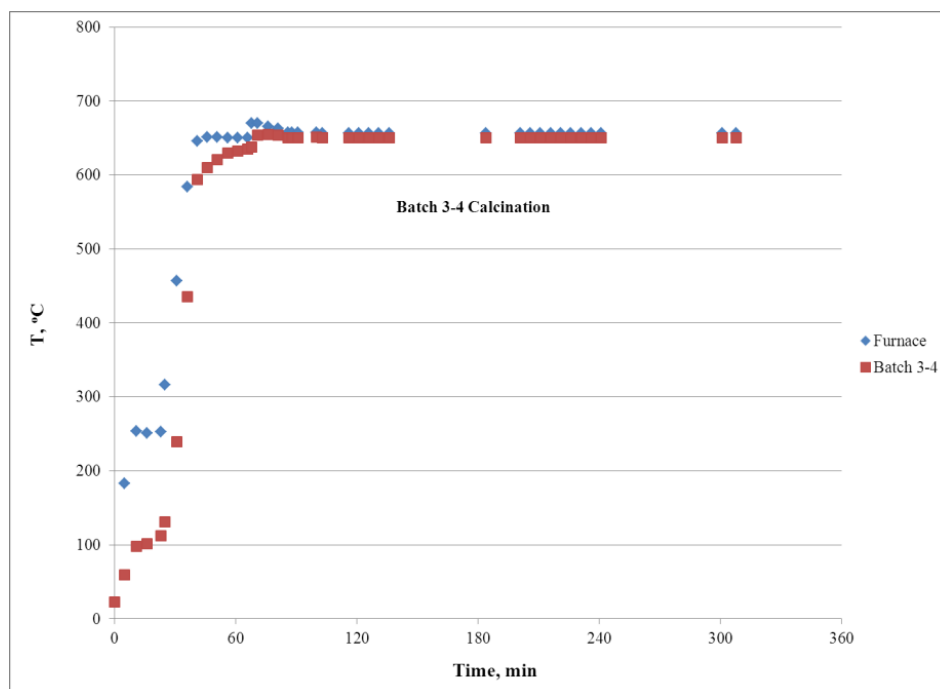


Figure B-7. Temperature Profile for Batch 3-4 Calcination

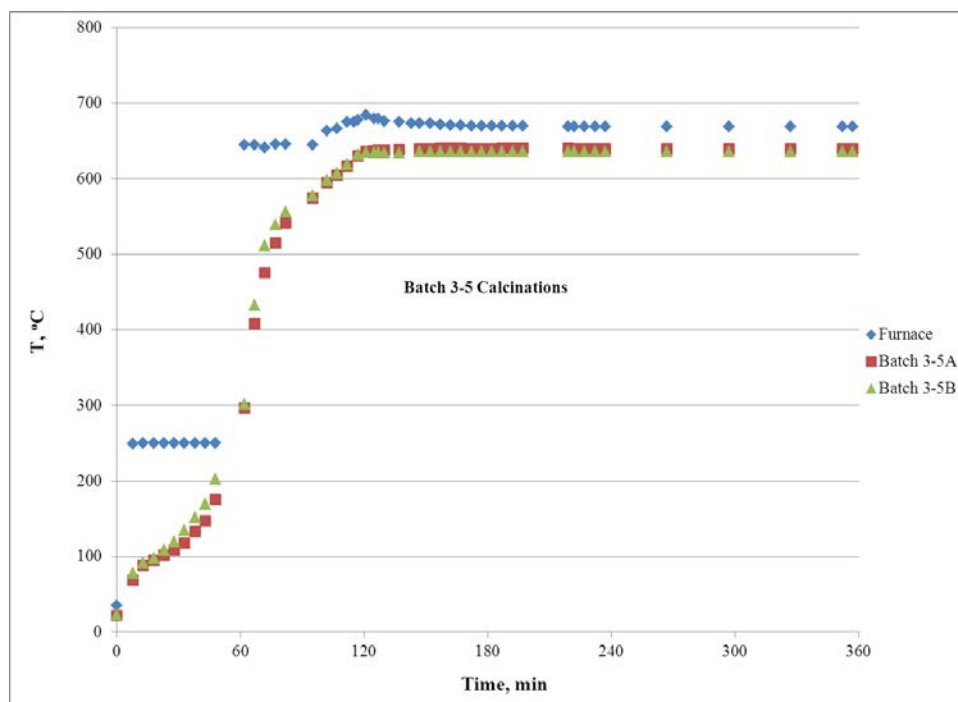


Figure B-8. Temperature Profiles for Batch 3-5 Calcinations

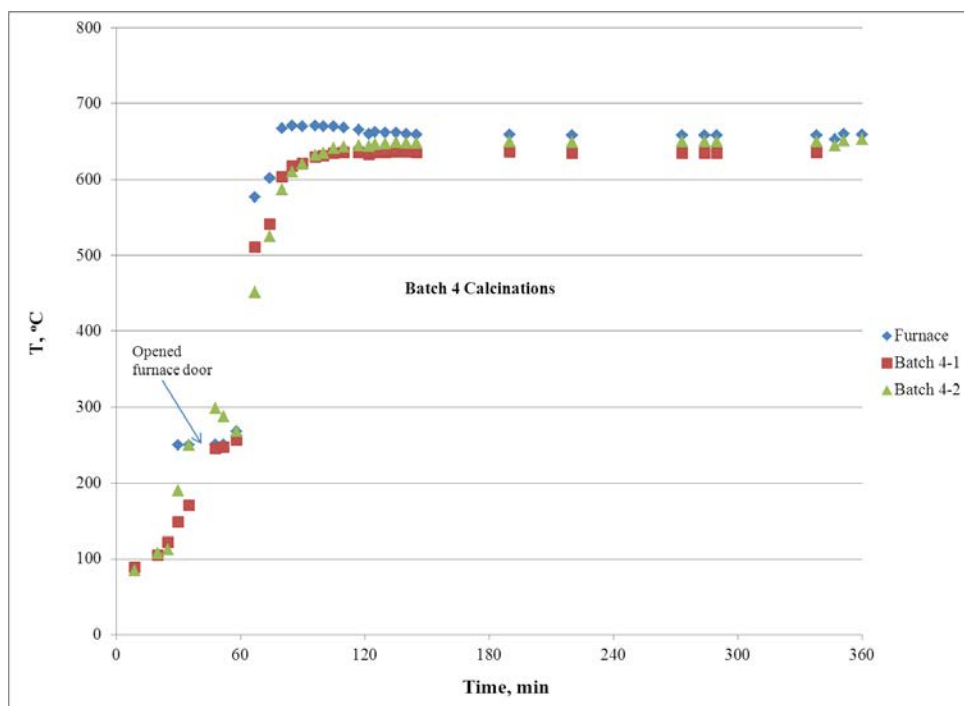


Figure B-9. Temperature Profiles for Batch 4 Calcinations

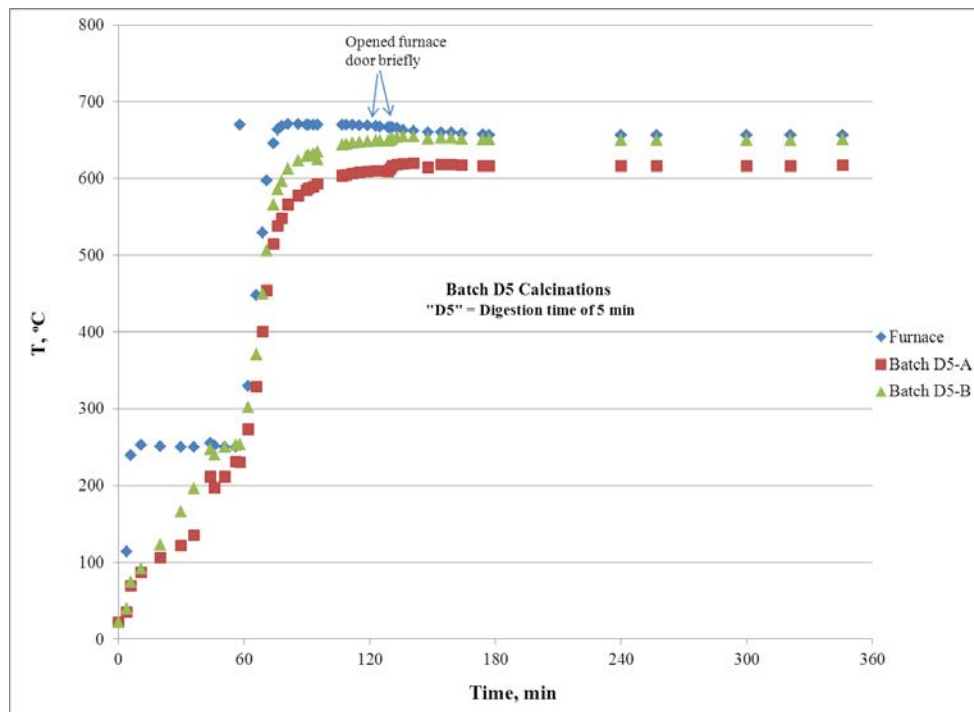


Figure B-10. Temperature Profiles for Batch D5 Calcinations

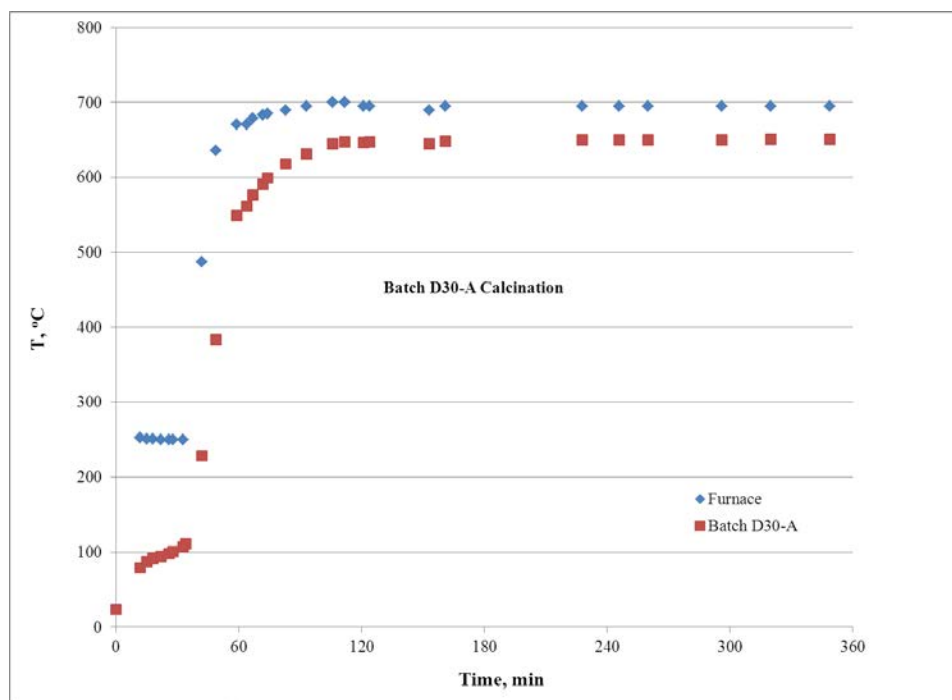


Figure B-11. Temperature Profile for Batch D30-A Calcination

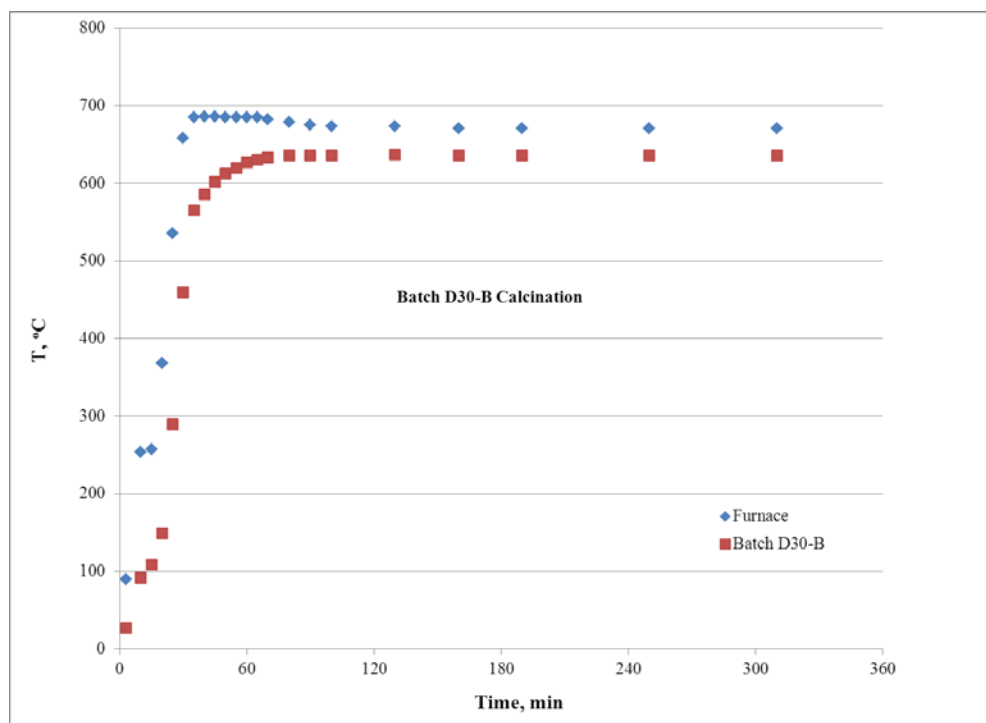


Figure B-12. Temperature Profile for Batch D30-B Calcination

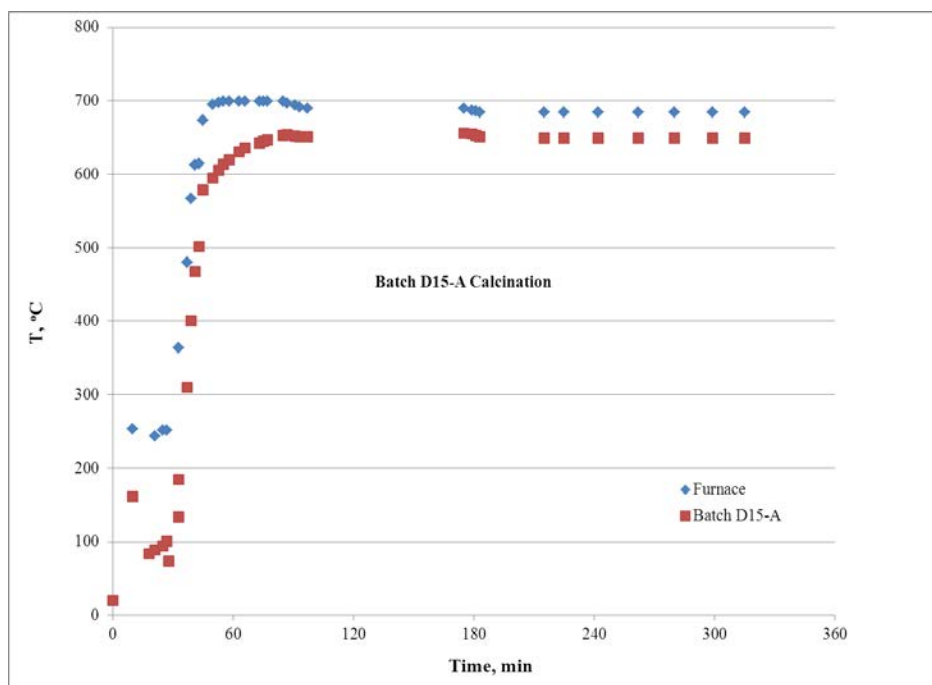


Figure B-13. Temperature Profile for Batch D15-A Calcination

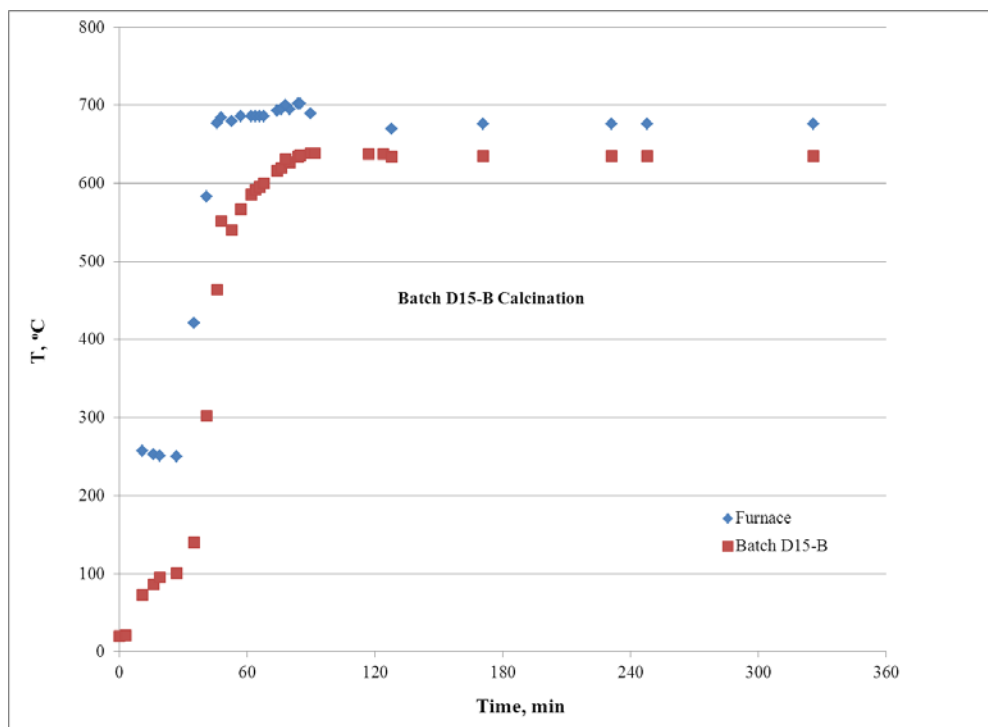


Figure B-14. Temperature Profile for Batch D15-B Calcination

Appendix C

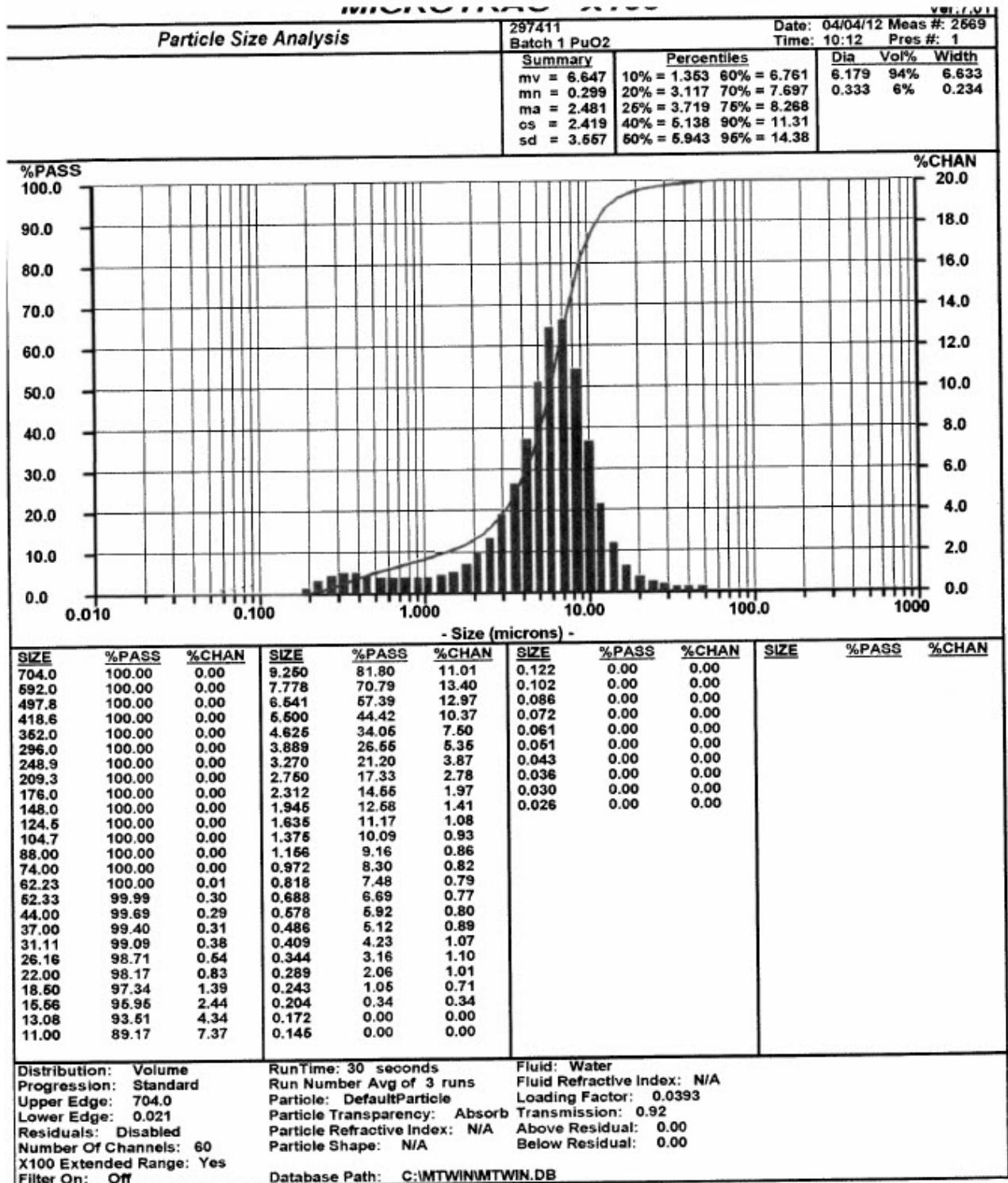


Figure C-1. Particle Size Analysis for Batch 1 PuO₂

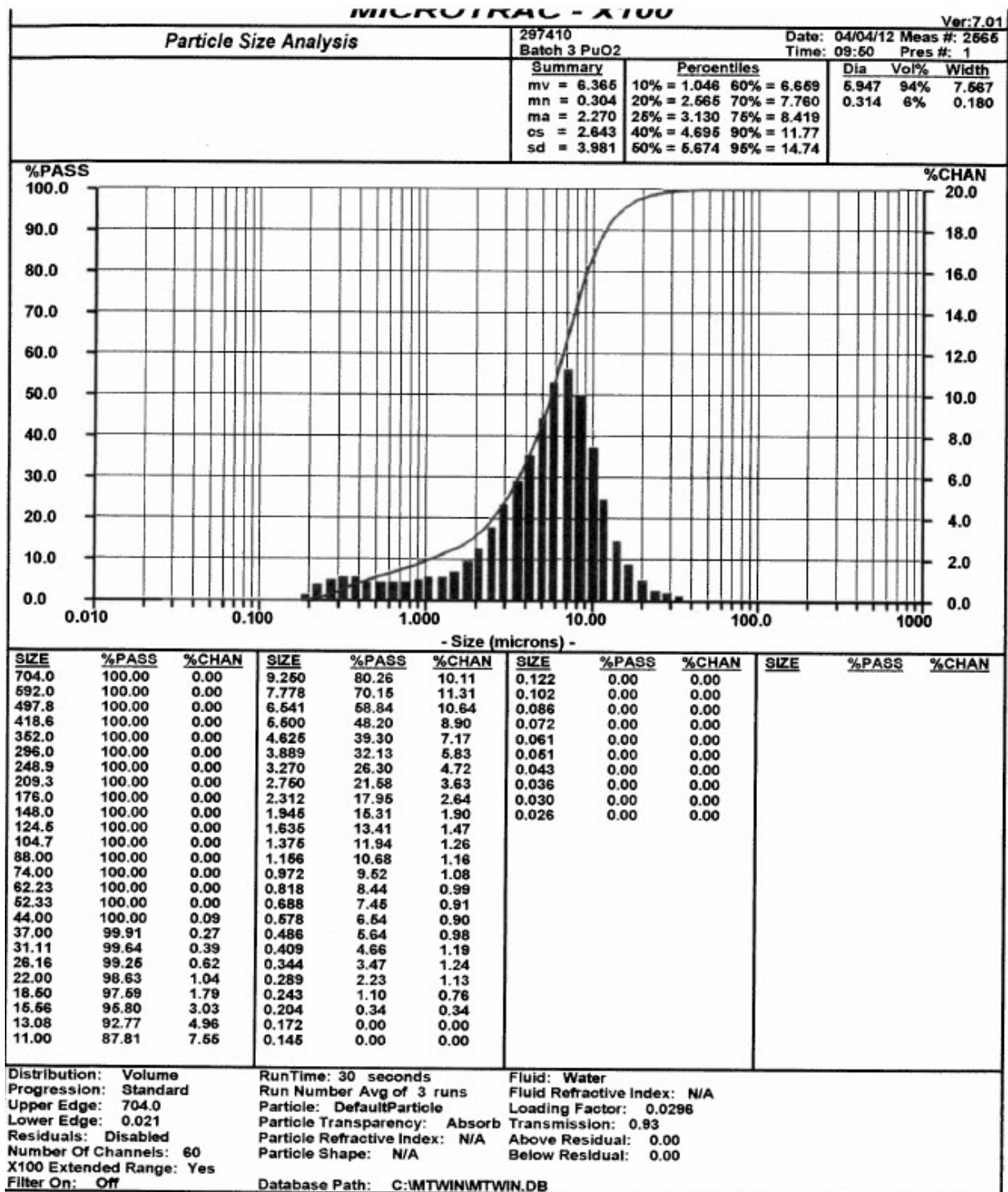


Figure C-2. Particle Size Analysis for Batch 3 PuO₂

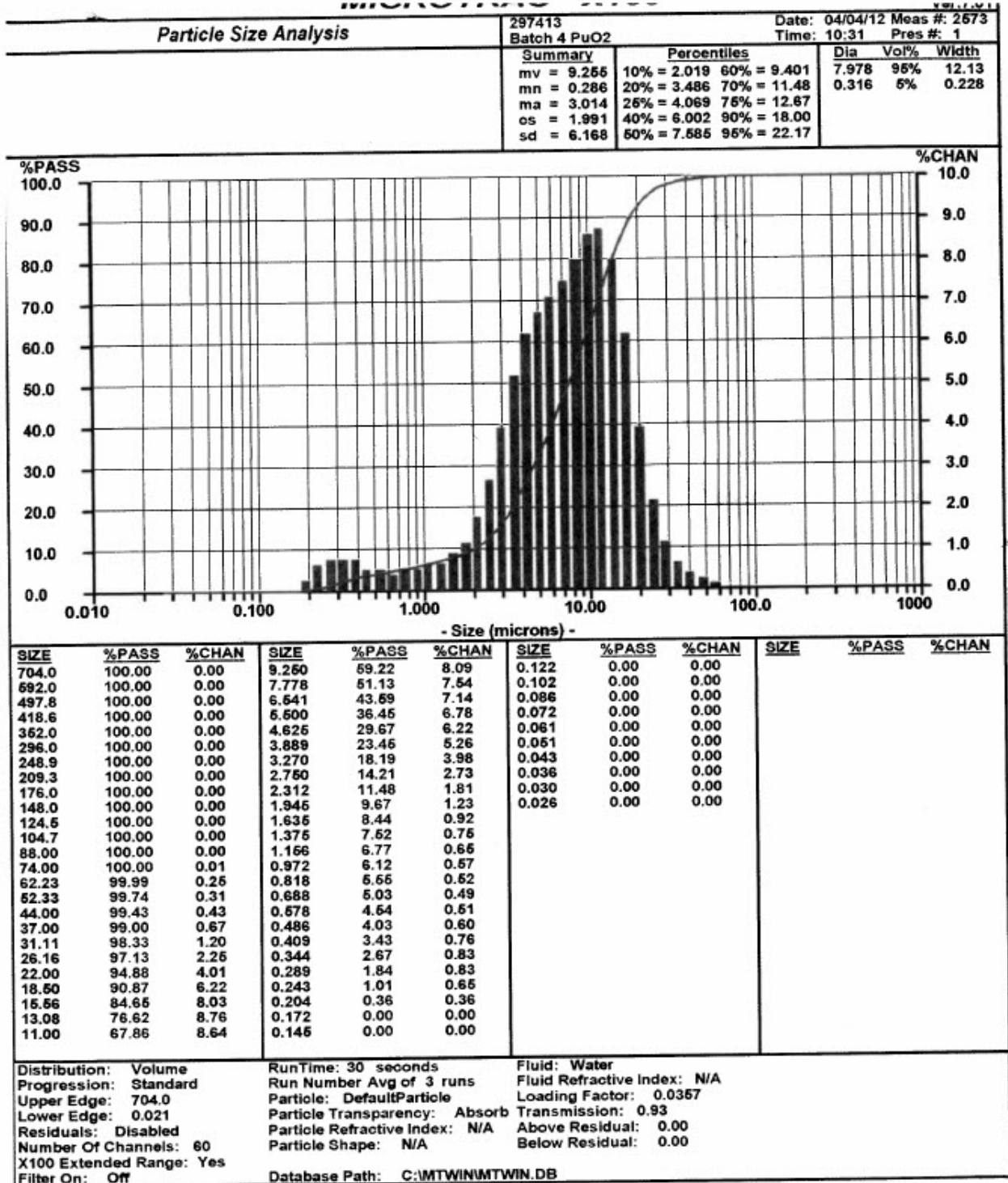


Figure C-3. Particle Size Analysis for Batch 4 PuO₂

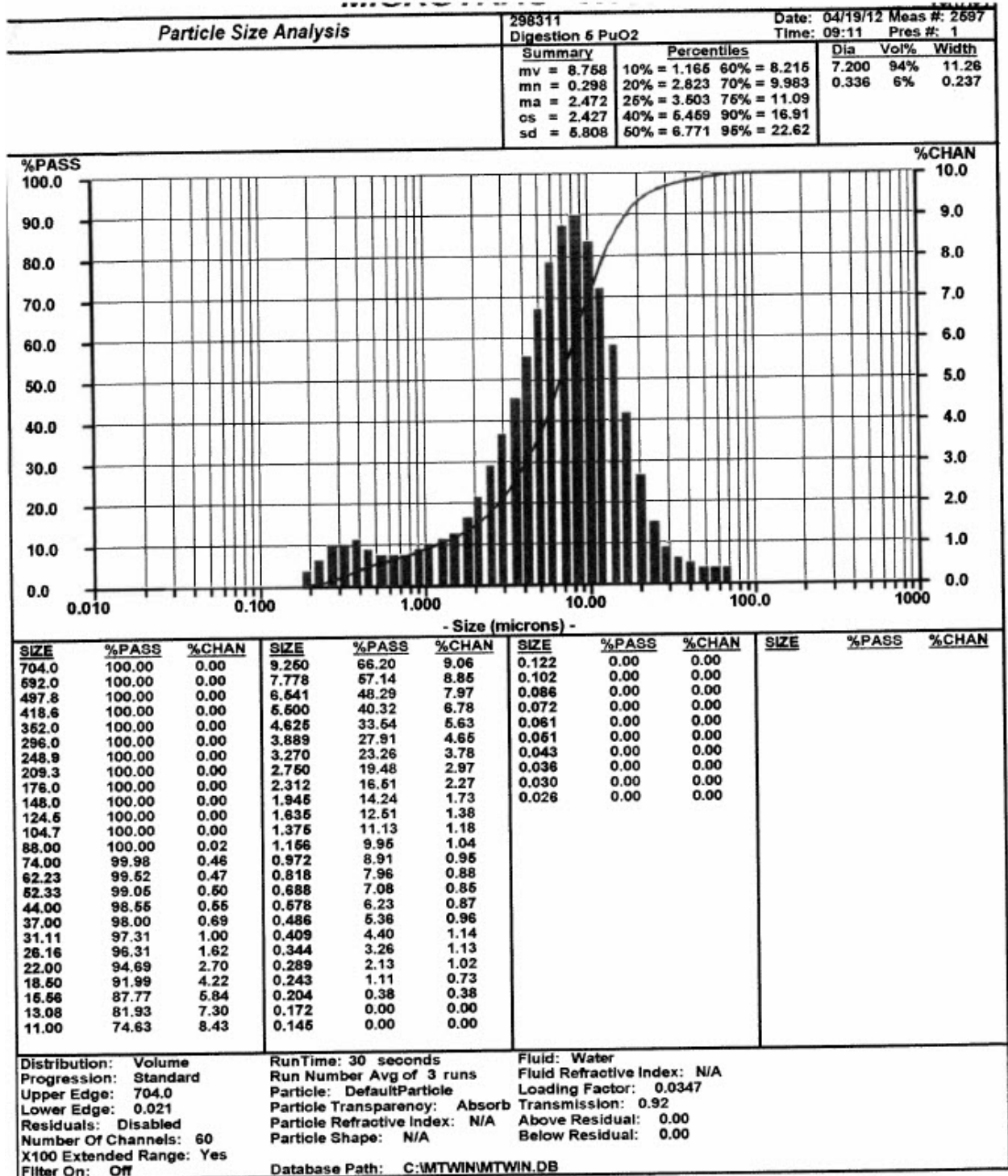


Figure C-4. Particle Size Analysis for Batch D5-A PuO₂

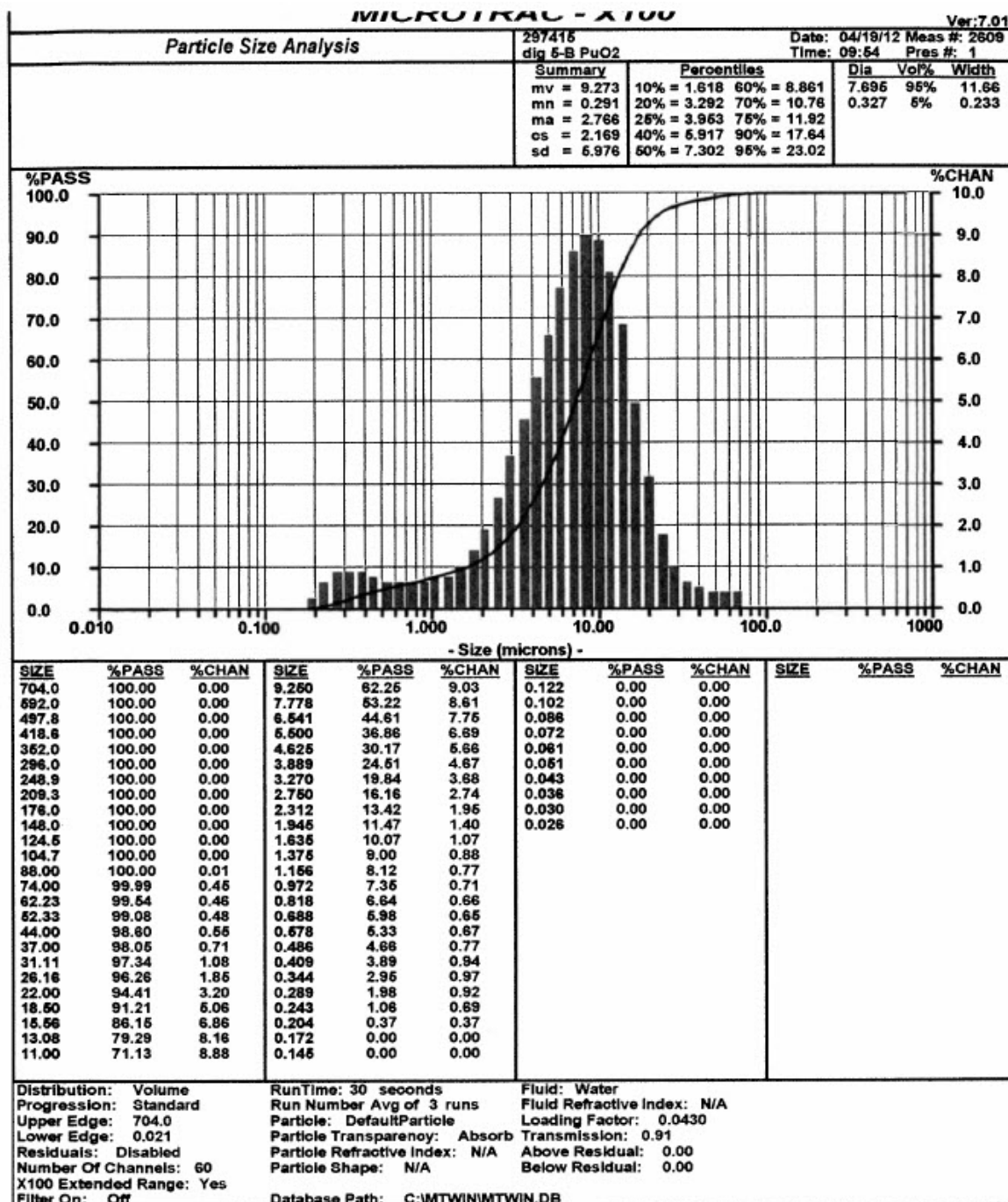


Figure C-5. Particle Size Analysis for Batch D5-B PuO₂

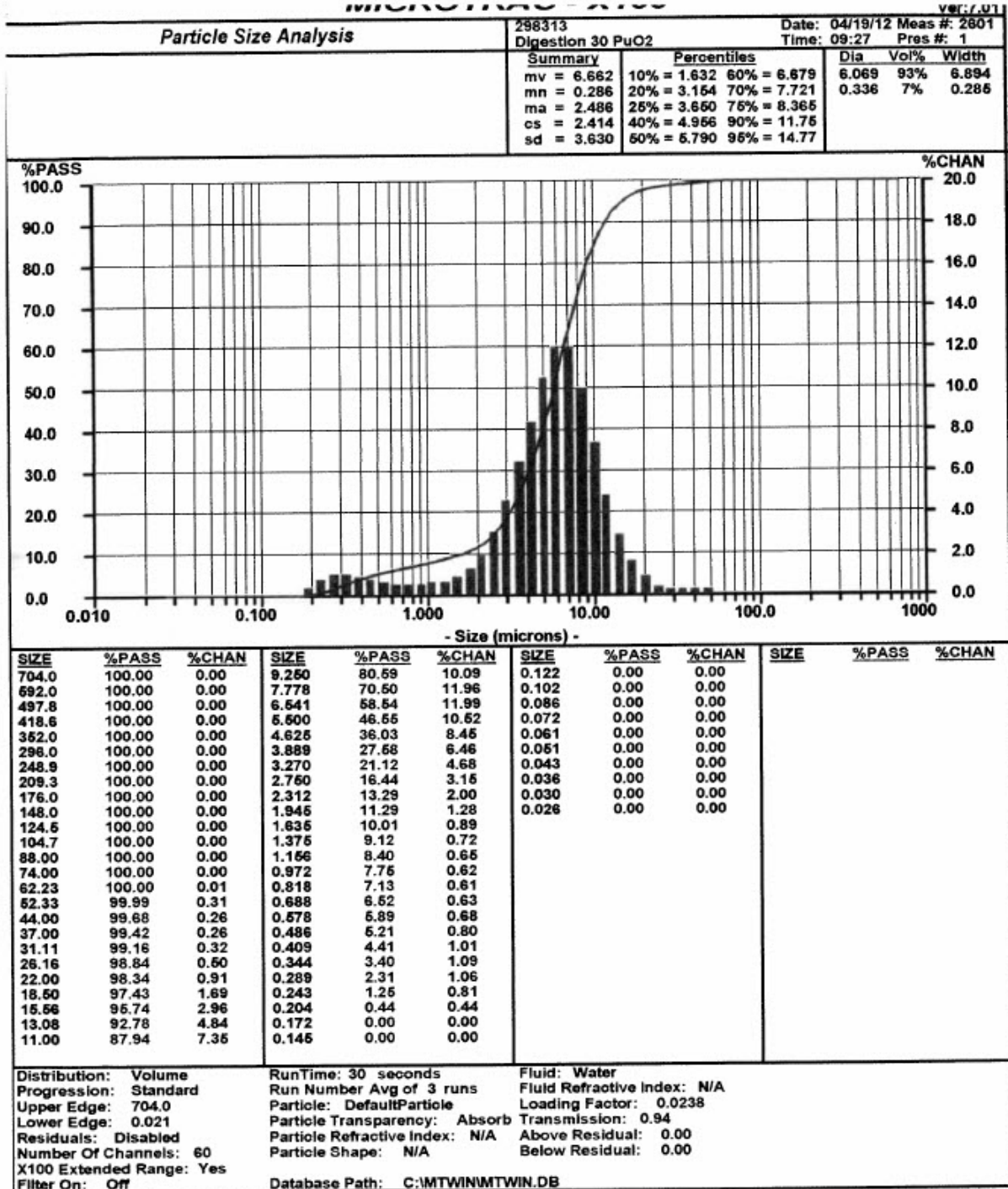


Figure C-6. Particle Size Analysis for Batch D30 PuO₂

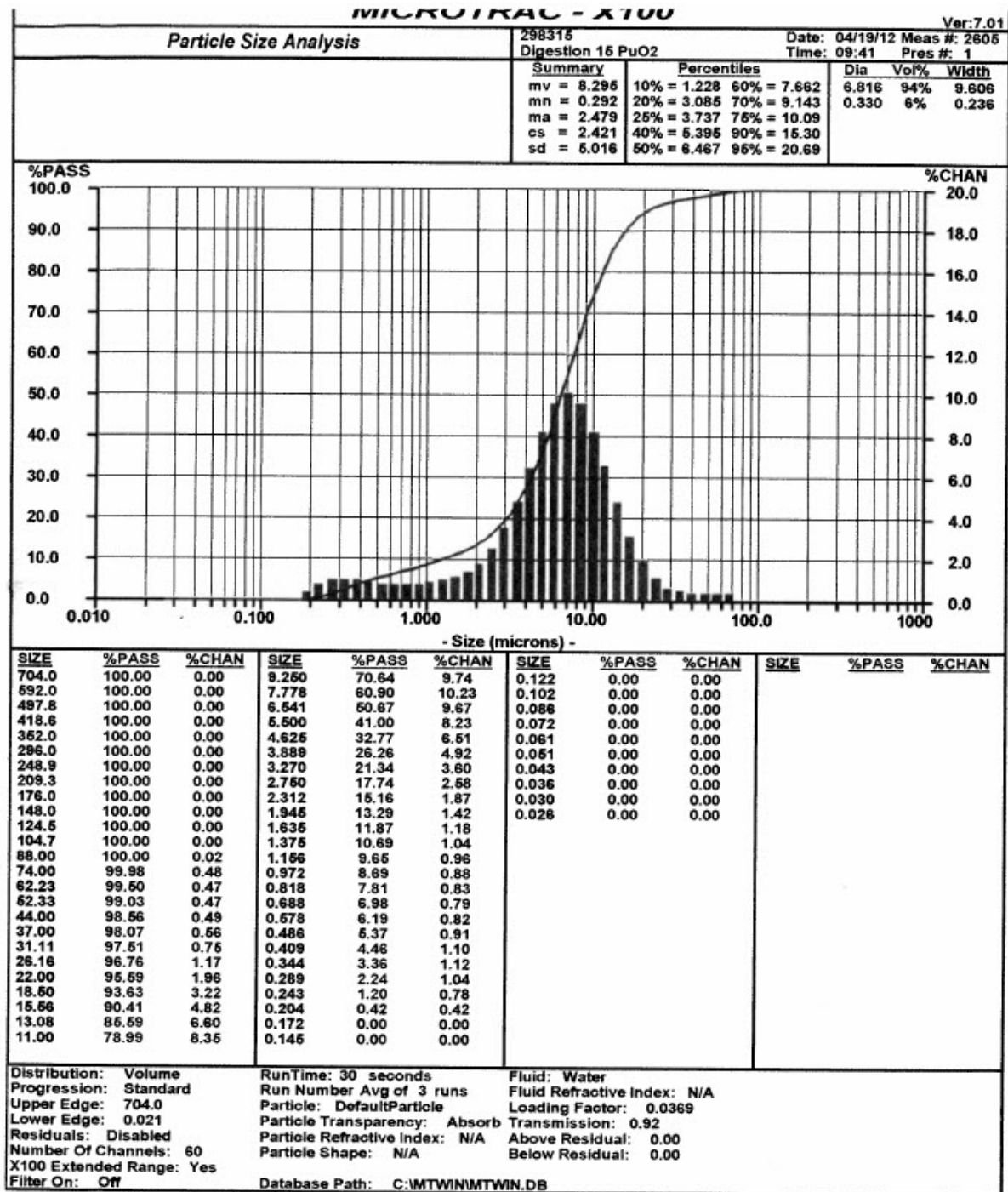


Figure C-7. Particle Size Analysis for Batch D15 PuO₂

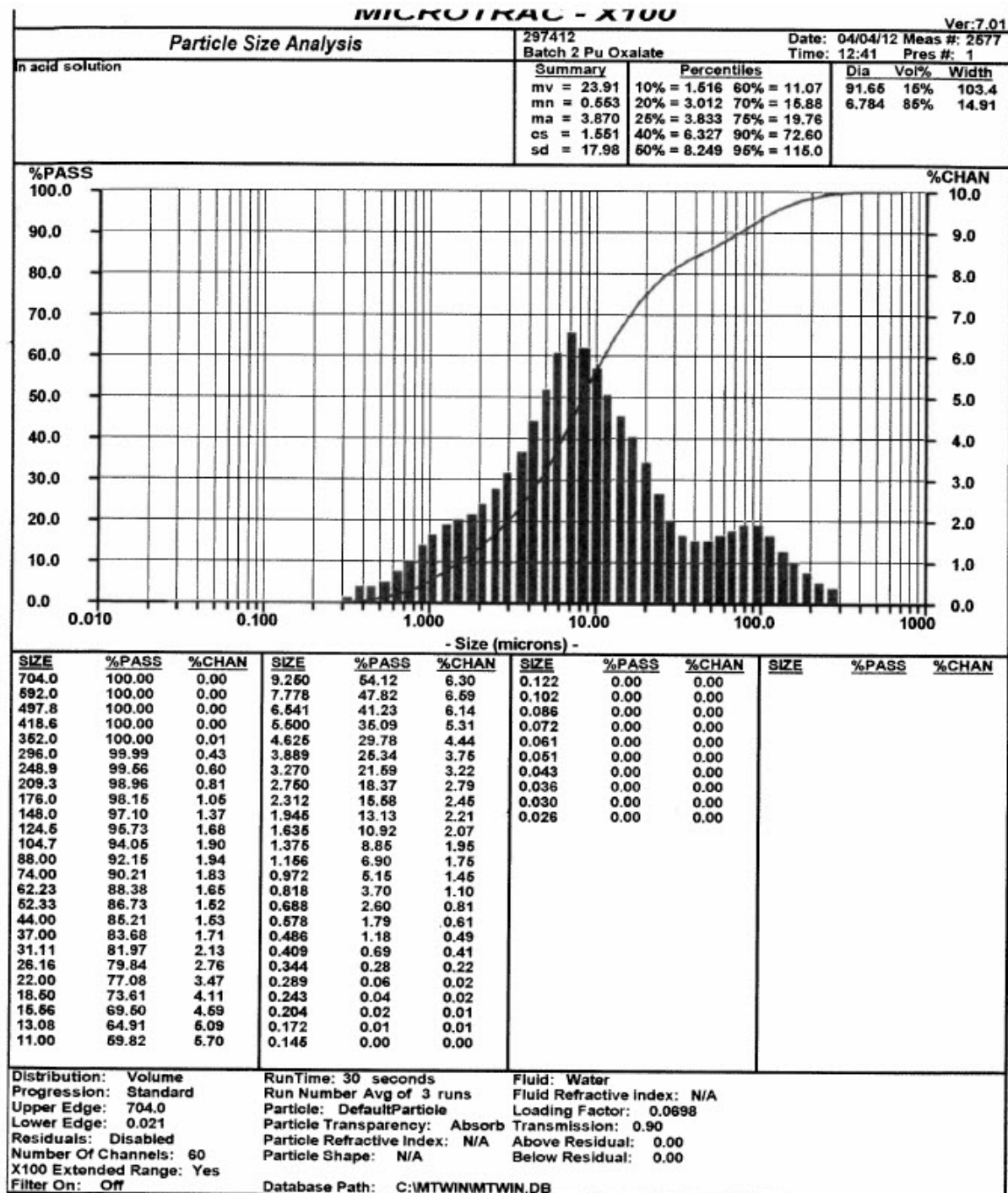


Figure C-8. Particle Size Analysis for Batch 2 Pu Oxalate

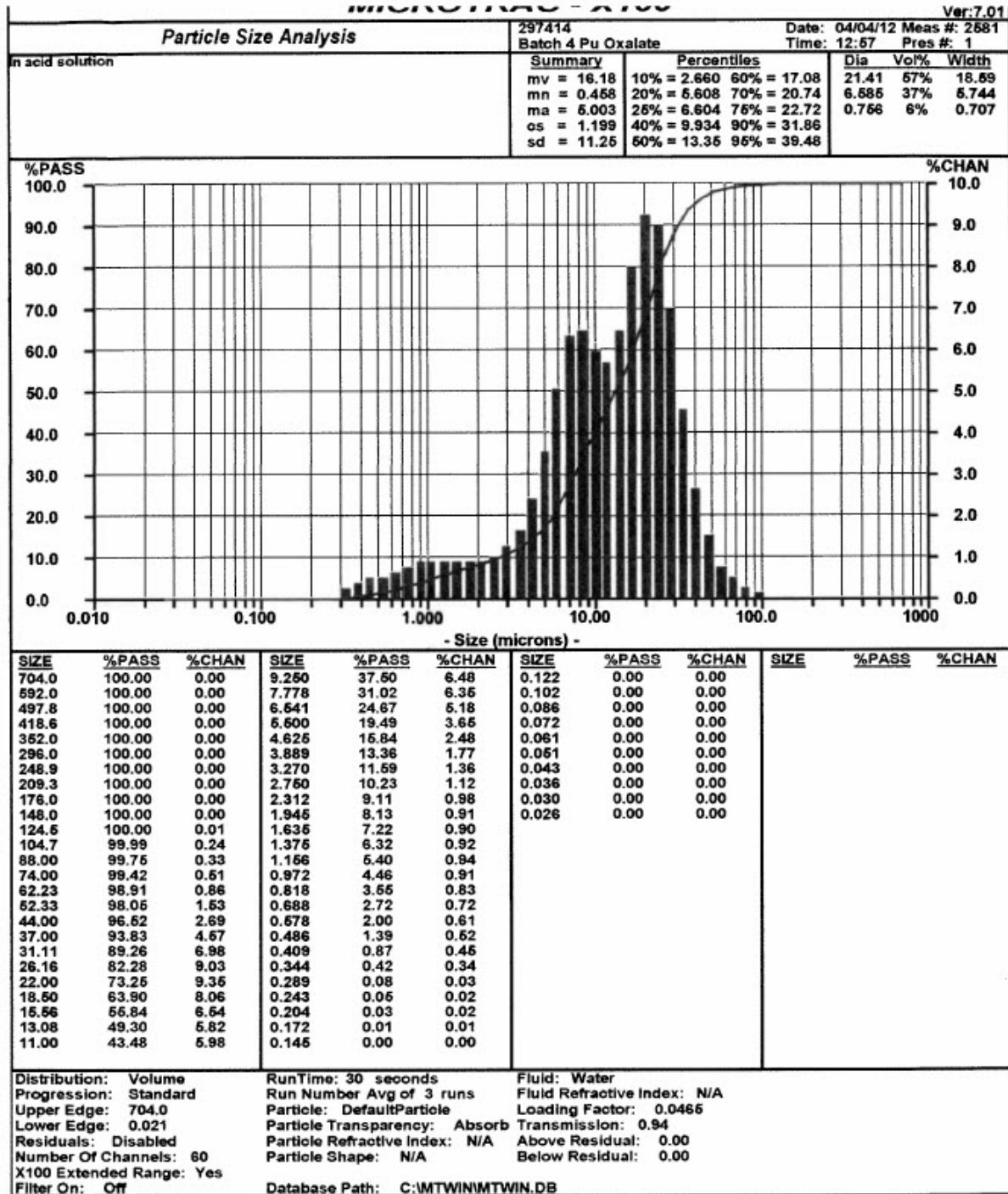


Figure C-9. Particle Size Analysis for Batch 4 Pu Oxalate

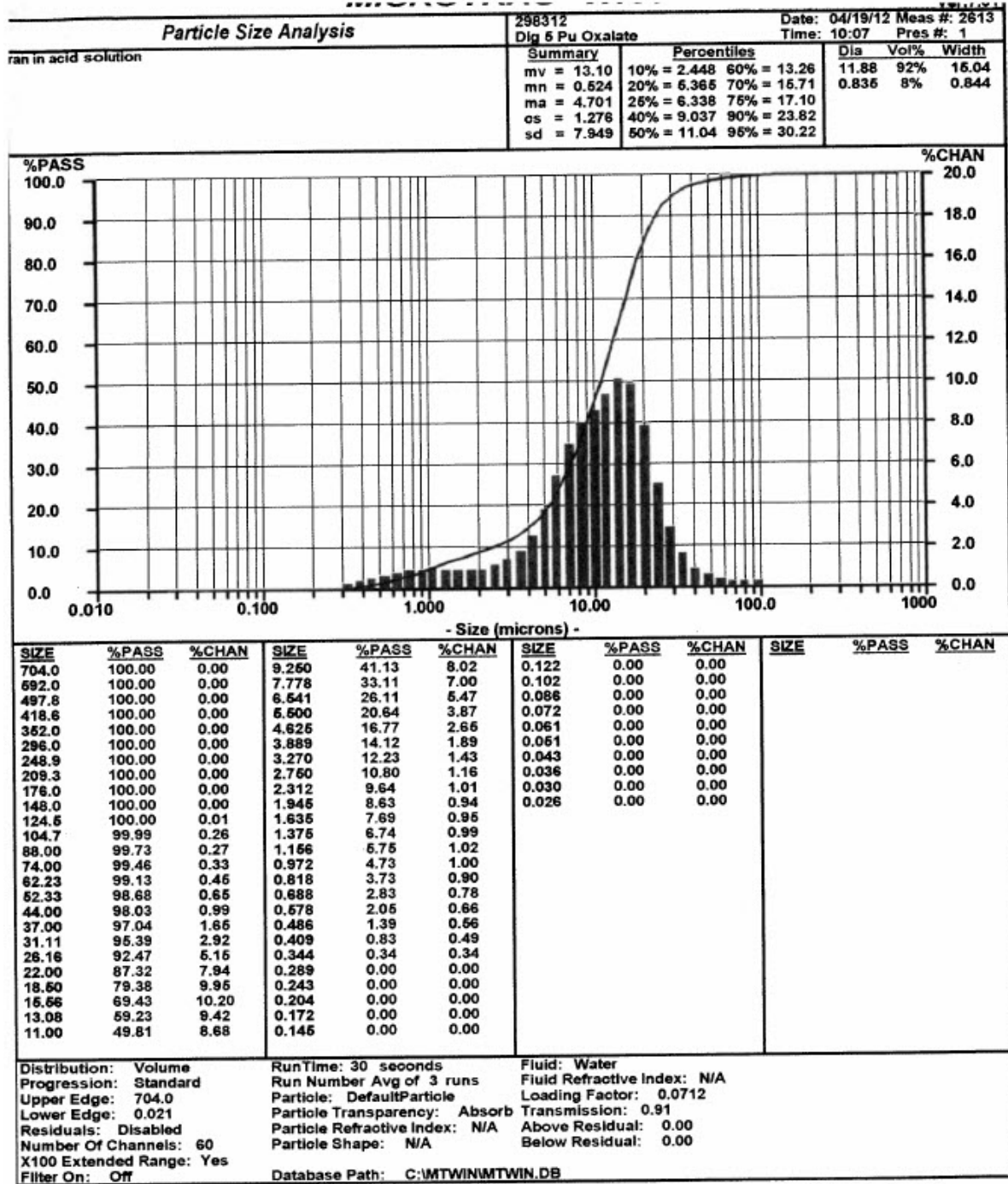


Figure C-10. Particle Size Analysis for Batch D5 Pu Oxalate

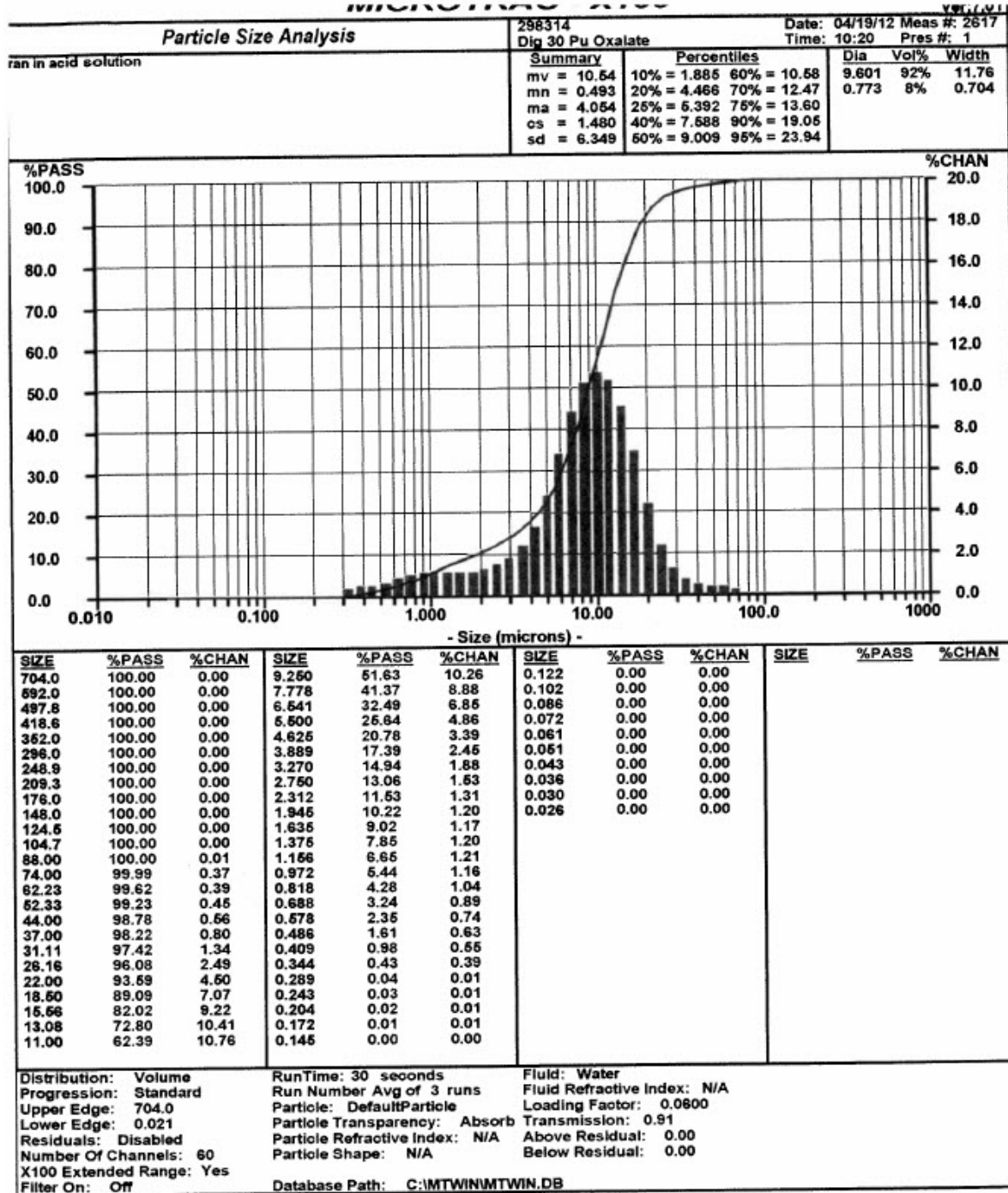


Figure C-11. Particle Size Analysis for Batch D30 Pu Oxalate

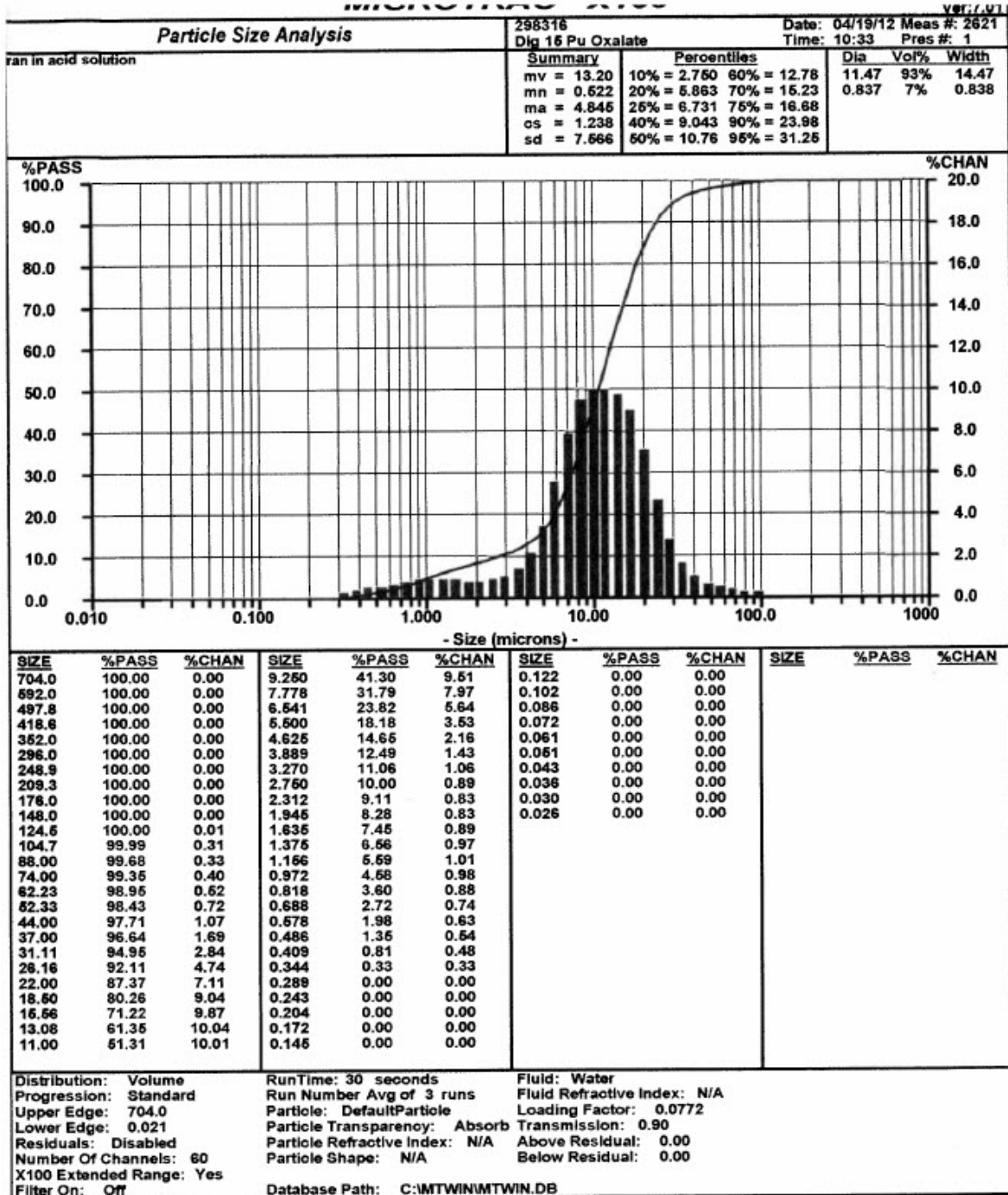


Figure C-12. Particle Size Analysis for Batch D15 Pu Oxalate

Distribution:

S. D. Fink, 773-A
K. M. Fox, 999-W
B. J. Giddings, 786-5A
C. C. Herman, 999-W
S. L. Marra, 773-A
F. M. Pennebaker, 773-42A
W. R. Wilmarth, 773-A
E. A. Kyser, 773-A
T. S. Rudisill, 773-A
R. A. Pierce, 773-A
J. H. Scogin, 773-A
M. C. Thompson, 773-A
W. E. Daniel, 999-W
W. D. King, 773-42A
C. A. Nash, 773-42A
M. L. Crowder, 773-A
K. M. L. Taylor-Pashow, 773-A

Records Administration (EDWS)

C. Wilson, 773-A

W. E. Harris, 704-2H
J. B. Schaade, 704-2H
G. J. Zachman, 225-7H
P. B. Andrews, 704-2H
S. J. Howell, 221-H
W. G. Dyer, 704-2H
M. J. Swain, 703-H
M. J. Lewczyk, 221-H
J. L. O'Conner, 704-2H
S. L. Hudlow, 221-H
W. H. Clifton, 704-2H
K. P. Burrows, 704-2H
K. J. Gallahue, 221-H
J. E. Therrell, 704-2H
J. W. Christopher, 704-2H
R. H. Smith, 704-2H
R. R. Livingston, 730-2B
D. Stimac, 730-2B
S. A. Thomas, 703-46A